Bull Volcanol (2003) 65:385–404
DOI 10.1007/s00445-002-0264-8

RESEARCH ARTICLE

Gloria Vaggelli · Lorella Francalanci · Giovanni Ruggieri · Silvia Testi

Persistent polybaric rests of calc-alkaline magmas at Stromboli volcano, Italy: pressure data from fluid inclusions in restitic quartzite nodules

Received: 19 February 2002 / Accepted: 18 November 2002 / Published online: 8 February 2003

Abstract A fluid-inclusion study has been performed on quartzite nodules of stromboli volcano hosted by calc-alkaline lavas of both the Strombolicchio (200 ka) and Paleostromboli II (60 ka) periods. The nodules are mainly composed of quartz crystals with subordinate plagioclase and K-feldspar. Small interstitial minerals such as plagioclase, K-feldspar, clinopyroxene, biotite, and quartz are also found, together with glass. Muscovite, epidote and zircon occur as accessory minerals. Different quartzite nodules occur: (1) equigranular polygonal granoblastic quartzite nodules forming a polygonal texture with clear triple points; (2) inequigranular polygonal granoblastic quartzite nodules; and (3) break-up nodules with strongly resorbed quartz. These quartzites are restites from partial melting, involving felsic crustal rocks at the magma/wall rock contact. Restitic quartz re-crystallises at variable and generally high temperatures, leading to the formation of quartzites with different textures. Quartz grains contain five types of fluid inclusions distinguished on the basis of both fluid type and textural/phase relationships at room temperature. Type I are two-phase (liquid+vapour) CO_2-rich fluid inclusions. They are primary and subordinately pseudosecondary in origin and have undergone re-equilibration processes. Type II mono-phase/two-phase (vapour/liquid+vapour) CO_2-rich fluid inclusions are the most common and, based on their spatial distribution and shape, they can be divided into two subclasses: type IIa and type IIb. Type II inclusions are secondary or pseudosecondary and they are assumed to have formed after decrepitation of type I inclusions and cracking of the host quartz. Type III inclusions are mono-phase (vapour); they possibly contain CO_2 at very low density and surround the inner rims of quartz grains. Type IV two-phase silicate-melt inclusions contain glass±CO_2-rich fluid. Some of them are cogenetic with type II inclusions. Finally, type V two-phase (liquid+vapour) aqueous inclusions are both vapour-rich and liquid-rich aqueous inclusions. Microthermometric experiments were performed on both type I and II inclusions. Type I inclusions homogenise to liquid between 20 and 30.5 °C. Type IIa inclusions homogenise to vapour in the 24 to 30 °C range, with a maximum peak of frequency at 29 °C. Type IIb inclusions also homogenise to vapour between 14 and 25 °C. There appears to be no difference in homogenisation temperature distribution between the Strombolicchio and Paleostromboli II samples. The trapping pressures of the fluid inclusions have been obtained by combining the microthermometric data of the Strombolicchio and Paleostromboli II samples with the pressure–temperature–volume (i.e. density) characteristics for a pure CO_2 system. The data on the early inclusions (type I) suggest an important magma rest at a pressure of about 290 MPa (i.e. about 11-km depth). Type IIa CO_2 inclusions suggest that a second magma rest occurred at a pressure of about 100 MPa (i.e. about 3.5-km depth), whereas type IIb inclusions were trapped later at a shallower depth during the final magma upwelling. No pressure/depth differences seem to occur between the Strombolicchio and Paleostromboli II periods, indicating the same polybaric rests for the calc-alkaline magmas of Stromboli, despite their significantly different ages. This persistence in magma

Editorial responsibility: T. Druitt

G. Vaggelli
C.N.R. Istituto di Geoscienze e Georisorse, Sezione di Firenze,
Via La Pira 4, 50121 Firenze, Italy

L. Francalanci
Dipartimento di Scienze della Terra, Università di Firenze,
Via La Pira 4, 50121 Firenze, Italy

L. Francalanci (✉) · S. Testi
Dipartimento di Scienze della Terra,
Università degli Studi di Firenze, Via La Pira 4,
50121 Firenze, Italy
e-mail: lorella@unifi.it
Tel.: +39-55-2757502
Fax: +39-55-290312

G. Ruggieri
C.N.R.,
Istituto di Geoscienze e Georisorse, Via Moruzzi 1,
56124 Pisa, Italy

stagnation conditions from 200 to 60 ka suggests a similar plumbing system for the present-day Strombolian activity.

Keywords Stromboli · Calc-alkaline magmas · Fluid inclusions · Melt inclusions · Quartzite nodules · Pressure data · Polybaric rests

Introduction

Stromboli is an active stratovolcano erupting shoshonitic to high-K calc-alkaline basalts by a persistent, moderate "Strombolian" activity. A great deal of research has been focused on rocks and volatiles from this activity in order to understand how it works, which parameters play an active role in the "Strombolian" activity, and when the more violent eruptions occur. One of the main problems, which has still to be solved, concerns the rest pressures of the magma, which entails a knowledge of the depth of occurrence of the evolutionary processes which lead to the present-day activity. It is of fundamental importance to determine whether a single magmatic reservoir exists or a number of reservoirs at different depths (e.g. Giberti et al. 1992; Ripepe et al. 1993; Allard et al. 1994; Bonaccorso et al. 1996; Harris and Stevenson 1997a, 1997b; Francalanci et al. 1999; Rosi et al. 2000).

The geochemical and petrological variations in the rocks erupted at Stromboli over time, from about 200 ka to the present day, indicate the presence of at least two magmatic reservoirs at different depths within the crust (Francalanci et al. 1989, 1993), but no geobarometer has ever confirmed this hypothesis or given us a precise pressure value. Data on CO_2 fluid inclusions can provide some constraints on pressure and hence on the depth at which the inclusions were formed. In particular, the density of the CO_2 inclusions and the pressure/depth relation can be obtained from the trapping temperature, which can be either assumed or determined by an independent geothermometer.

At Stromboli, fluid inclusions were found in the quartzite nodules only, which are exclusively hosted by calc-alkaline lavas of 200 and 60 ka. The results of the microthermometric and microanalytical study performed on CO_2 and silicate-melt inclusions are therefore reported in this paper. The results will be interpreted and discussed in the light of the different rest pressures of the calc-alkaline magmas. These pressures could also be considered as possible resting places for the magma feeding the present-day volcanic system.

Volcanological and petrological background

Stromboli belongs to the Aeolian volcanic arc (southern Tyrrhenian Sea, Italy) which consists of seven subaerial Quaternary volcanoes and several submarine volcanoes occurring above a north-westward-dipping Benioff zone (McKenzie 1972; Knott and Turco 1991). It lies on an 18-km-thick continental crust (Morelli et al. 1975) and rises from a depth of about 2,500 m beneath sea level to an elevation of 924 m above sea level.

The volcanological history of the subaerial part of Stromboli, from about 100 ka to the present day, is characterised by the following six main periods of activity: (1) Paleostromboli I, (2) Paleostromboli II, (3) Paleostromboli III, (4) Vancori, (5) Neostromboli, and (6) Recent period (Hornig-Kjarsgaard et al. 1993). The Strombolicchio neck, located about 1.7 km NE of Stromboli, belongs to the same volcanic system and represents the oldest subaerial rocks of the volcano (204±25 ka; Gillot and Keller 1993).

The rock compositions vary from calc-alkaline (mainly basaltic andesites) to potassic alkaline (potassic trachybasalts and shoshonites), through high-K calc-alkaline (high-K basalts to high-K andesites) and shoshonitic (shoshonitic basalts to few trachytes). Strombolicchio lavas are calc-alkaline, as are Paleostromboli II rocks which are mainly made up of lava flows. During Paleostromboli I and Paleostromboli III, lavas and pyroclastic rocks with mainly high-K calc-alkaline composition were erupted. The Vancori period was mostly characterised by shoshonitic lavas, whereas Neostromboli rocks are thin scoriaceous lava flows with potassic-alkaline composition. The rocks of the Recent period ("*Pizzo Sopra la Fossa*" pyroclastic cone, "*San Bartolo*" lava flows and the products of present-day activity) are younger than 5.6±3.3 ka (Gillot and Keller 1993), and they are represented by lavas and pyroclastic deposits with shoshonitic and high-K basaltic compositions (Francalanci et al. 1989, 1993; Hornig-Kjarsgaard et al. 1993).

The present-day activity takes place from three main craters on a terrace 750 m a.s.l. inside the "*Sciara del Fuoco*" depression. The regular activity consists of continuous, mild explosions at variable intervals, with ejection of bombs, black scoriae, blocks, lapilli and ash. The regular Strombolian activity is periodically broken by lava flow eruptions and by more violent explosions than usual, in which the lapilli and ashes can reach the coastal zones and sometimes built-up areas. During the more violent explosions, small amounts of a volatile-rich and phenocryst-poor (less than 5 vol%) magma is erupted as light pumice, together with the normal phenocryst-rich (about 50 vol%) and degassed magma (Bonaccorso et al. 1996; Francalanci et al. 1999; Rosi et al. 2000) which is erupted as black scoriae and bombs.

Detailed studies of the petrology and magmatological history of Stromboli volcano have allowed to identify the variable and complex processes of magma evolution, such as simple fractional crystallisation, crustal assimilation, mixing and a combination of these processes, probably occurring in reservoirs sited at various depths within the crust (Francalanci et al. 1988, 1989, 1993).

Aeolian crustal basement

Geophysical data and geodynamic considerations suggest that the terranes belonging to the Kabilo-Peloritano-

Calabride domain constitute the crustal basement of the Aeolian volcanic arc (Gasparini et al. 1982). The Kabilo-Peloritano-Calabride group is made up of a series of tectonic units representing different portions of an original Hercynian continental crust with its Meso-Cainozoic sedimentary cover (Zvi Ben et al. 1990).

These terranes are well exposed in the Calabrian Arc, where the exposed tectono-stratigraphic sequence is made up of high- to medium-grade metamorphic rocks in granulitic through amphibolitic to greenschist facies, as well as granitoid igneous rocks and unmetamorphosed sedimentary rocks bounded by tectonic contacts (Schenk 1980, 1989, 1990). The crustal sequence outcropping in south Calabria, at the "*Le Serre*" Massif (Maccarone et al. 1983; Caggianelli et al. 1991), may be considered as representative of the crustal basement of the Aeolian Arc.

The Serre Massif is represented by a sequence of four tectonic units (Del Moro et al. 1986) consisting, from bottom to top, of the following: (1) the Bagni Unit, made up of Palaeozoic metapelites equilibrated under greenschist facies conditions; (2) the Castagna Unit, including gneiss and paragneiss in amphibolite facies and micaschists with rare granitoids; (3) the Polia-Copanello Unit, including rocks in granulite/amphibolite facies represented by garnet–sillimanite gneisses and fels, amphibolitic gneisses with intercalations of basic/ultrabasic rocks and marbles and, finally, diorites and tonalites; felsic and basic granulites also occur on the Tyrrhenian side, east of Pizzo Calabro; (4) the Stilo Unit, including late Hercynian granodiorites, granites and tonalites intruded in Palaeozoic metapelites and paragneiss and covered by Mesozoic sedimentary deposits.

Analytical techniques

Microscopic observations have been carried out on doubly polished sections of about 100–300 μm. In addition to transmitted optical petrography, a JEOL JSM-840 scanning electron microscope (United States Geological Survey, Reston, VA) was used to improve detection of the inclusions.

The microthermometric investigations on CO_2 inclusions were performed with Linkam THM600 heating-freezing stages (at the CNR-IGG in Florence and Pisa). The stages were calibrated with pure H_2O synthetic fluid inclusions, and natural pure CO_2 inclusions. Accuracy is estimated in the order of ±0.2 °C within the examined temperature range.

To check for the presence of other gases besides CO_2, Raman spectroscopic analyses (Microdill-28) were performed on some selected inclusions at the Vrije Universiteit, Amsterdam (Burke and Lustenhouver 1987).

Microprobe analyses of the silicate-melt inclusions were obtained with both an automated ARL SEMQ at the USGS in Reston, Virginia (USA) and a JEOL JXA-8600 superprobe at the CNR-IGG in Florence. The analyses were carried out with 15-kV accelerating voltage, 10-nA beam current, and the Bence and Albee (1968) matrix correction routine. In order to avoid or minimise alkali loss, we used a defocused beam (10 μm) and a lower counting time for Na, measuring both Na and K at the beginning of each analysis, as experimentally tested by Vaggelli et al. (1999). Natural silicate minerals were mostly used as primary standard, whereas trachytic obsidian CFA-47 from the Phlegrean Fields (Metrich and Clocchiatti 1989) was used as secondary standard to test glass analyses. Further analytical details, together with precision and accuracy, are reported in Vaggelli et al. (1999).

Petrography of quartzite nodules

The samples studied (Table 1) are represented by quartzite nodules hosted by calc-alkaline basaltic andesite lavas of both the Strombolicchio neck (about 200 ka) and the Paleostromboli II period (hereafter called the PSTII; about 60 ka). The latter were collected from the "*Omo lavas*" cropping out at La Petrazza. The size of the xenoliths varies from a few to about 10 cm. They are mainly made up of quartz grains of different shapes and sizes. A few samples also contain resorbed K-feldspar (STR239l) and/or plagioclase (STR239l and STR239z1) as primary phases. Small plagioclase, K-feldspar, clinopyroxene, quartz and biotite occur as rare interstitial phases, along with glass films. Muscovite, epidote and zircon occur as accessory minerals. The outer contact with host lavas is commonly sharp and characterised by the presence of a coronitic texture mainly constituted by prismatic clinopyroxene microcrystals, elongated perpendicular to the contact interface and, subordinately, by interstitial plagioclase, K-feldspar and glass.

Different types of quartz crystals were found: (1) large (several millimetres wide), dusty and irregularly shaped quartz porphyroblast (ReQ=relict quartz) with undulose extinction; (2) clear quartz grains of variable size (from a few hundred microns to several millimetres in width), with sharp and straight rims (RQ=re-crystallised quartz); (3) large, clear quartz grains (up to a few millimetres in width) very similar to RQ quartz but with a light, undulose extinction (LRQ=large re-crystallised quartz); (4) resorbed quartz grains with a dusty or clear appearance (MQ=melted quartz) which resemble ReQ, RQ and LRQ quartz grains. RQ and LRQ quartz grains may show triple junctions and polygonal textures and are also characterised by coronitic textures with quartz of new generation, as indicated by fine layers of tiny inclusions surrounding the crystal inner rims. The relatively large ReQ grains are sometimes replaced by smaller RQ crystals which grow within, or at the grain boundary of the ReQ grains.

Based on petrographic features, ReQ is interpreted to be a relict, strained and presumably metamorphic quartz only partially re-crystallised; on the contrary, RQ and LRQ quartz are the products of thermal re-crystallisation and, finally, MQ represents both ReQ, RQ and LRQ after a final partial melting process (see below).

Table 1 Petrographic description of the restitic quartzite nodules (symbols from Kretz 1983)

Sample	Texture	Occurrence of quartz type[a]	Interstitial phases and accessory minerals	Analysed inclusions
Strombolicchio calc-alkaline lavas (200 ka)				
STR257a	Medium equigranular granoblastic	RQ+LRQ	Pl, cpx	Type IIa
STR257b	Small/medium disequigranular banded granoblastic	ReQ+RQ	Cpx, ep, qtz, glass	-
STR257d	Small/medium disequigranular banded granoblastic	ReQ+RQ	Cpx, kfs, pl	Type I, type IVa
STR257e	Small/large disequigranular banded granoblastic	ReQ+RQ	Bt, cpx, ms	Type I, type IIa
STR257h	Small/medium disequigranular banded granoblastic	ReQ+RQ	Bt, cpx	Type I
STR257i	Medium equigranular granoblastic	RQ+LRQ	Cpx	Type IVa
STR257m	Medium equigranular granoblastic	RQ+MQ	Qtz, kfs, pl, cpx	Type I, type IVa
STR257o	Resorbed qtz	MQ	Kfs, cpx	-
STR257q	Resorbed qtz	MQ	Kfs, cpx	-
STR257r	Small/medium disequigranular banded granoblastic	ReQ+RQ	Glass, ep	-
STR257s	Small/medium disequigranular banded granoblastic	ReQ+RQ	Glass	Type IIa
STR257z1	Medium/large disequigranular banded granoblastic qtz+pl	ReQ+RQ	Bt, kfs, pl, cpx, zr	Type IVa
Paleostromboli II calc-alkaline lavas (60 ka)				
STR239d	Medium/large disequigranular banded granoblastic	ReQ+RQ	Glass, cpx	-
STR239e	Small/large disequigranular banded granoblastic	ReQ+RQ	Glass, cpx	Type I, type IIa, b
STR239f	Granoblastic	RQ+LRQ	Glass, qtz	Type I, type IIa, b
STR239j	Resorbed qtz	MQ	Kfs, cpx, qtz, glass	Type IVa
STR239k	Large equigranular granoblastic	RQ+LRQ	Qtz, cpx	Type I, type IIa
STR239l	Medium/large disequigranular banded granoblastic qtz+kf+pl	ReQ+RQ	Qtz, cpx	-
STR203	Quartz aggregates		-	Type IIa, type IVa

[a] ReQ, relict quartz; RQ, re-crystallised quartz; LRQ, large re-crystallised quartz; MQ, melted quartz; qtz, quartz; pl, plagioclase; kfs, K-feldspar; cpx, clinopyroxene; bt, biotite; ms, muscovite; ep, epidote; zr, zircon

According to their quartz-type occurrence, the quartzite nodules were divided into three groups.

1. Inequigranular polygonal granoblastic nodules with banded levels of ReQ and RQ quartz grains (Fig. 1a). These are characterised by rare and scattered triple points, by occasional MQ quartz crystals, and by the widespread presence of brown interstitial glass, often replacing the original triple junctions.
2. Equigranular granoblastic nodules with medium to large (up to a few millimetres wide) RQ and LRQ quartz crystals forming a solid granular and polygonal texture with clear triple points (Fig. 1b). Only STR257m is made up of RQ quartz crystals only, sometimes partially resorbed (MQ grains; Table 1).
3. Break-up nodules with MQ quartz grains which appear to be strongly resorbed, irregularly shaped and surrounded by glass or cristobalite microcrystals (Fig. 1c).

Fluid inclusions

Thirteen quartzite nodules were selected for fluid-inclusion studies, eight from the calc-alkaline lavas of Strombolicchio and five from the calc-alkaline lavas of "*Omo lavas*" (PSTII; Table 1). The quartz grains contain five types of fluid inclusions, distinguished on the basis of their textural/phase relationships at room temperature, homogenisation behaviour and fluid type (Fig. 2).

Type I inclusions (Fig. 3a–c) are two-phase, liquid+vapour (L+V) CO_2-rich inclusions and homogenise to the liquid phase. They are present in most sampled nodules but are rare in some samples. They are observed in RQ and LRQ quartz and sporadically (STR239e) in ReQ, in all nodule types (Table 1).

Type I inclusions usually occur as isolated inclusions or in clusters at the grain cores and rims of both PSTII and Strombolicchio samples; they can be considered primary in origin following the criteria of Roedder (1984), i.e. they were entrapped during quartz crystallisation. In STR257m sample only, the type I inclusions also occur along pseudosecondary trails (i.e. they formed when the host crystal fractures during its growth; Roedder 1984). Type I inclusions show mostly subspherical or negative crystal shape; subordinately they display elongated or irregular shapes. They are usually transparent and smaller than 20 μm. In all samples except STR257m, many relatively large (10–20 μm) and some small (<10 μm) type I inclusions show typical decrepitation features (fractures and small trails of inclusions extending from the original primary inclusions). In sample STR257m, however, the type I inclusions do not show decrepitation textures.

Type II inclusions are mono-phase vapour (V) or two-phase liquid+vapour (L+V) CO_2-rich inclusions and homogenise to the vapour phase. Although they are by far the most common inclusions and occur in equigranular, inequigranular granoblastic and break-up nodules (Fig. 3d), they are not equally distributed among the studied samples. There are quartz grains rich in these fluid

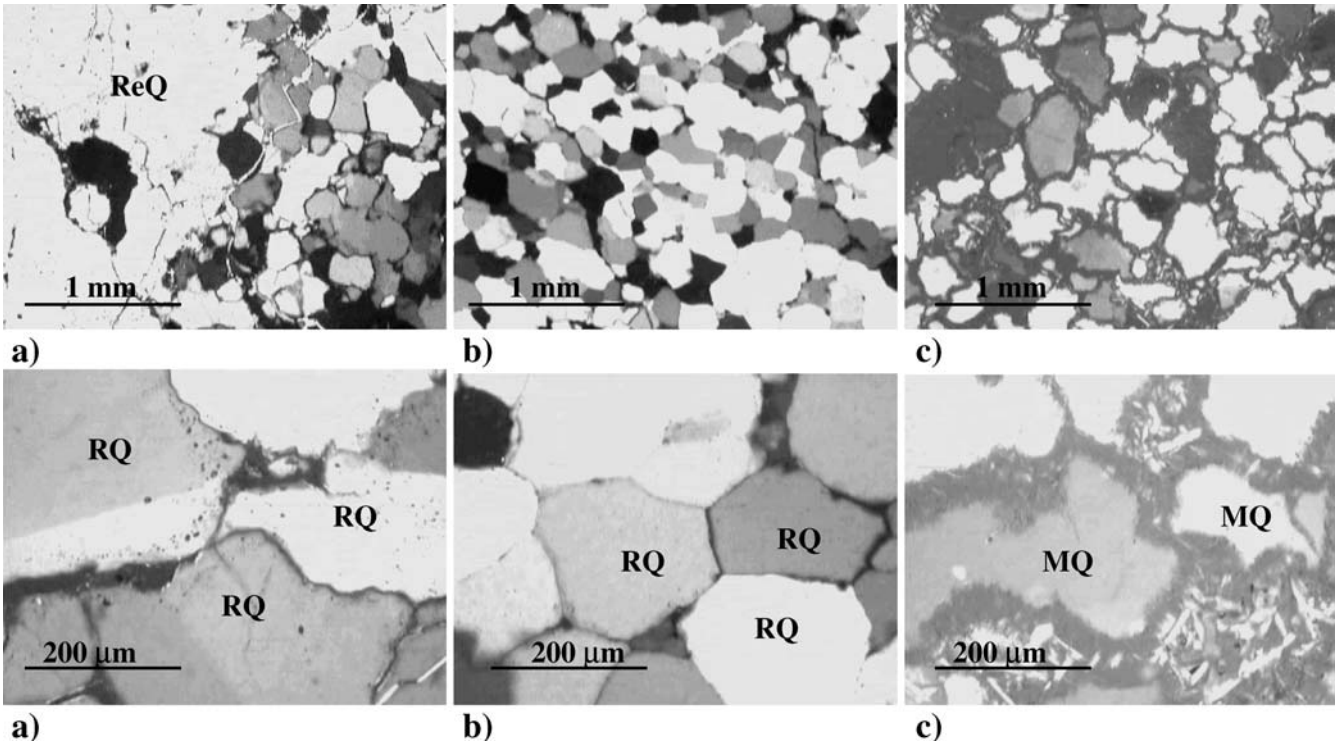

Fig. 1. **a** Transmitted light photomicrograph of inequigranular polygonal granoblastic nodules with bands of relict (*ReQ*) and re-crystallised (*RQ*) quartz grains. **b** Equigranular granoblastic nodules with medium/large (millimetres wide) re-crystallised quartz (*RQ*) crystals forming a solid granular and polygonal texture with clear triple points. **c** Break-up nodules with melted quartz (*MQ*) grains

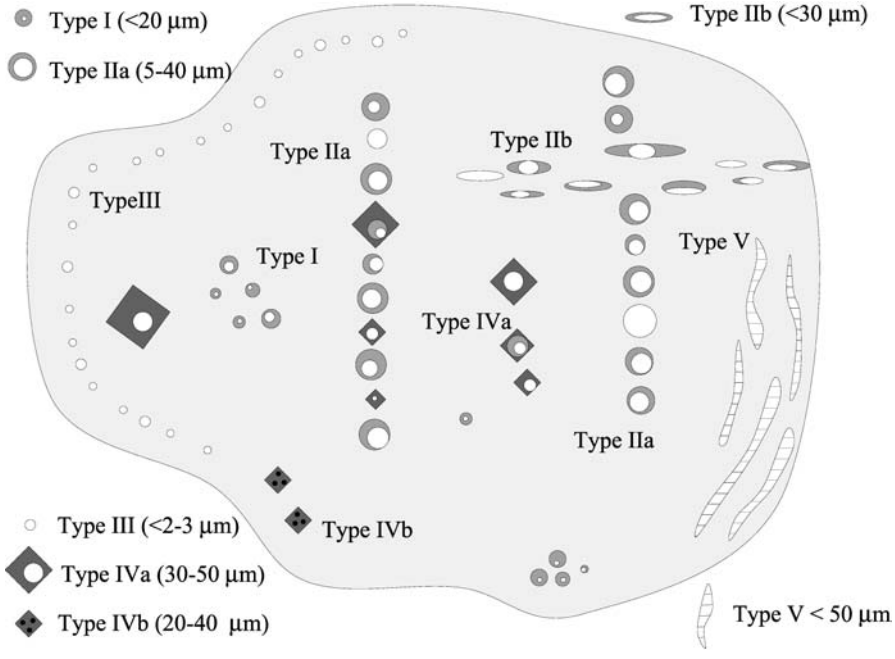

Fig. 2 Schematic representation of the identified fluid-inclusion types. *Open symbol*, CO_2 vapour, *light shading*, CO_2 liquid, *dark shading*, homogeneous glass, *dark shading* with *closed dots*, inhomogeneous glass, *horizontal lines*, water

inclusions and others lacking inclusions. In STR257m no type II inclusions were observed.

Based on their spatial distribution and shape, the type II inclusions can be further divided into two classes: type IIa and type IIb. Type IIa inclusions occur both at PSTII and at Strombolicchio. They are dark, mostly subspherical, have a rather inconstant diameter of 5–40 μm, and are sometimes associated with silicate-melt inclusions (type IVa). They arrange along planes which resemble old microfractures which are now well healed. Conse-

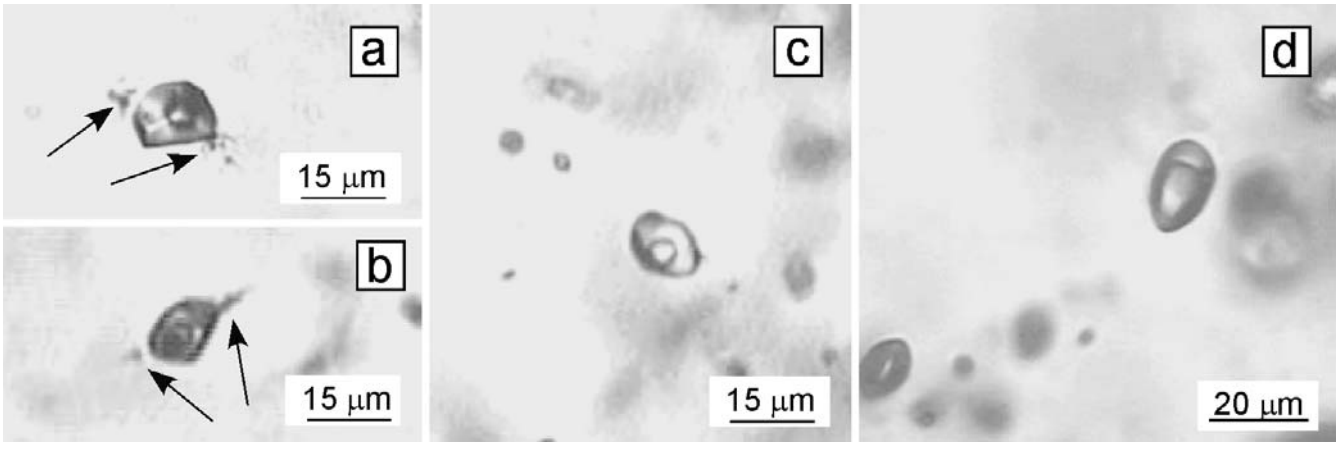

Fig. 3a–d Photomicrographs of type I and II CO_2 inclusions hosted in quartz nodules. **a, b** Primary type I inclusion in STR257d nodule showing decrepitation features (healed fractures indicated by *arrows*). **c** Primary type I inclusion with regular shape in STR257m nodule. **d** Secondary type II inclusions along a healed fracture in STR257e

quently, type IIa inclusions show a "mature aspect" (Roedder 1984). Indeed, during healing, the cavity of the inclusions tends to a minor surface energy and, from an initially irregular and/or elongated shape, acquires a subspherical and/or negative crystal shape. Type IIb are present only in PSTII and have elongated, subcylindrical shapes with a maximum size of 30 μm, although the most common size is 10–15 μm. They intersect and slightly displace the type IIa inclusions, showing a less "mature aspect". Type IIb can therefore be considered younger than type IIa but both populations are clearly secondary in origin (i.e. they formed after the complete crystallisation of the host quartz and following a crystal fracture with subsequent healing).

Type III are present only in RQ and LRQ quartz grains; they are tiny (a few μm) and mono-phase inclusions. They are mostly dark and subspherical, surrounding the inner rims of the RQ and LRQ quartz grains but they are not found along triple points (Fig. 1a). They occur only at Strombolicchio in inequigranular banded nodules and subordinately in equigranular granoblastic nodules. Type IIa trails appear to stop at the intersection with type III. Unfortunately, this type of inclusion does not show any phase changes during the cooling/heating runs. Nevertheless, we assume that they contain CO_2 at very low density.

Type IV two-phase or three-phase silicate-melt inclusions contain glass±CO_2 liquid/vapour (G+V±L) and occur in RQ and LRQ quartz. They can be divided into type IVa and type IVb, according to the glass type.

Type IVa are the most common silicate-melt inclusions, are transparent, contain variable proportions of homogeneous glass±CO_2 liquid/vapour, and usually have a negative crystal (β-form) shape. They are present in both the PSTII and Strombolicchio samples. The most common size is 30–50 μm. Detailed back-scattered SEM electron images suggest that crystallisation of the host occurred on the inclusion walls but that it was minimal in the analysed samples. Unidentified trapped/daughter silicic minerals are sometimes observed in samples STR203, STR239k and STR257e. Type IVa inclusions occupy well-healed microfractures, together with type IIa CO_2 inclusions, but some larger inclusions occur in isolation or in small clusters. According to their occurrence and distribution, they can be considered either primary in origin with respect to RQ and LRQ quartz, or secondary in origin when associated with type IIa inclusions along trails.

Type IVb silicate-melt inclusions are much less common; they are dark brown–dusty and drab in plane-transmitted light, and are generally as large as type IVa inclusions; however, no textural relationships allow us to univocally relate them to type IVa. This type of inclusion is found in quartz grains from PSTII. Back-scattered SEM electron images show that these inclusions contain two immiscible glasses: a darker glass forms ca. 1-μm spheres (the pale globules in the SEM back-scattered image), surrounded by a more transparent glass (the dark matrix). Semi-quantitative SEM–EDS analyses show that the pale microspheres have significantly more Fe and Ca than the matrix glass.

Type V two-phase fluid inclusions are both vapour-rich and liquid-rich aqueous inclusions. They are relatively less abundant than type II CO_2 inclusions and definitely secondary in origin, occurring along trails with an "immature aspect" in both Strombolicchio and PSTII quartzite nodules.

In addition to the above fluid-inclusion types, many dark inclusions, similar to type III inclusions, were also observed in RQ and ReQ. These dark inclusions differ from type III inclusions in that they are of larger size (up to 50 μm), they mostly occur in the quartz cores, and they are sometimes associated with decrepitation features. In RQ they show primary texture (isolated inclusions) whereas in ReQ they also occur along secondary/pseudosecondary trails. These inclusions, which apparently do not contain any visible fluid, are interpreted to

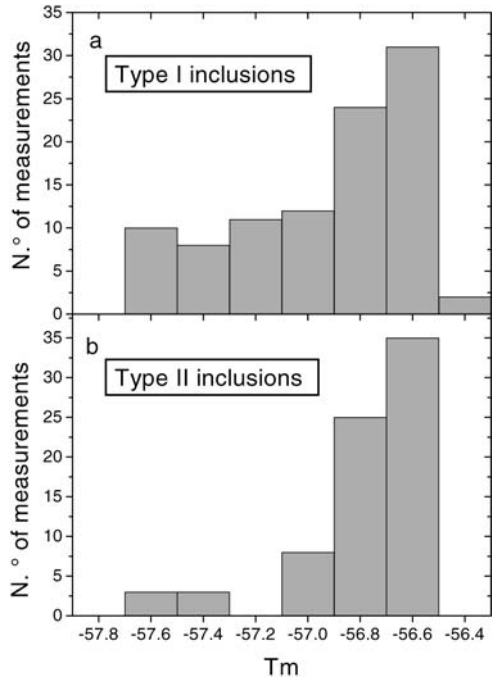

Fig. 4 Temperature of melting of the carbonic phase (Tm) for type I inclusions (a) and type II inclusions (b) in both Strombolicchio and Paleostromboli II. N° of measurements = number of analysed inclusions

represent open inclusions which lose their trapped fluid during decrepitation phenomena (see below).

Microthermometry

Microthermometric experiments were performed on type I, II and III CO_2 inclusions but no thermometric data were derived from the type III inclusions. No experiments were carried out on silicate-melt (type IV) and aqueous (type V) inclusions.

Type I CO_2 inclusions were analysed in four samples from Strombolicchio and three from PSTII. The melting temperature of the carbonic phase (Tm) of the type I inclusions, obtained by warming previously frozen inclusions, was found to be in the range −57.7/−56.4 °C (Fig. 4a). In most type I inclusions (around 70%), Tm was in the range of −56.4/−56.9 °C, around the triple point of CO_2.

The CO_2 homogenisation temperatures to the liquid phase (ThL) for each single sample of type I inclusion are shown in Fig. 5. Type I inclusions homogenise between about 20 and 30.5 °C (Fig. 5). Most of the samples containing inclusions with decrepitation features, whether from Strombolicchio (STR257d and STR 257e) or PSTII (STR239e and STR239k), display a wide ThL range with one or more maximum frequency peaks (Fig. 5). Relatively high ThL variations are usually found at the scale of the single fluid-inclusion assemblage. The other samples show narrower ThL ranges, with inclusions showing decrepitation textures—between 26 and 30 °C in sample STR257h, and in the 23–25 °C range in sample STR239f where only a very few type I inclusions occur. Usually there is a rough positive correlation between the Th and the size of inclusions.

In the sample containing type I inclusions without re-equilibration textures (STR257m), the ThL ranges between 27 and 30.5 °C, with a well-defined maximum at about 30 °C (Fig. 5).

Type II inclusions were studied in four samples of PSTII and three of Strombolicchio (Fig. 6). The temperatures of melting of the carbonic phase (Tm) of type II inclusions range from −57.6 to −56.5 °C (Fig. 4b) but most type II inclusions (around 90%) are in the range −56.5/−56.9 °C.

In the samples from Strombolicchio, type IIb inclusions are absent and type IIa inclusions display ThV in the 25 to 29 °C range, with maximum frequencies at 26 °C (sample STR257s) and at 29 °C (samples STR257a and STR257e). Type IIa and type IIb both occur in the PSTII samples and their ThV are in the 24 to 30.5 and 14 to 25 °C range respectively. In most PSTII samples (STR239e, STR239k and STR203), the type IIa inclusions show a maximum of frequency at about 29 °C whereas sample STR239f is characterised by a maximum at 27–28 °C. In sample STR203 the CO_2 bubble of type IVa (glass+CO_2) inclusions shows ThV similar to that of the type IIa CO_2 inclusions trapped in the same sample. Type IIb CO_2 inclusions do not display a clear frequency peak.

Type III inclusions showed no phase changes during the cooling/heating runs and could not be analysed by Raman because of their small size. It was, therefore, impossible to determine their composition. The dark appearance of these inclusions, however, is typical of gas-rich inclusions. We would also suggest that this gas phase is constituted by very low-density CO_2.

Compositions of the fluid inclusions

Most of the fluid inclusions show Tm close to the triple point of CO_2, indicating that the fluid trapped in these inclusions is nearly pure CO_2. In the inclusions displaying relatively low Tm, some amounts of other gases (N_2 and/or CH_4) may be present. For type I and II inclusions, an attempt was made to estimate the amount of CH_4 and N_2 from the Tm and Th of single inclusions, using the method of Thiery et al. (1994). The maximum concentration of CH_4 and N_2 in type I inclusions was found to be around 5.0 and 11.0 mol% respectively. Using the same method, the maximum CH_4 and N_2 contents in type II have been estimated at 5.0 and 7.0 mol% respectively. Raman analyses on some selected type II inclusions (from sample STR203) detected no gas other than CO_2; no Raman investigations could be carried out on type I inclusions because of their small size.

Liquid water may be present as a thin film wetting the walls of type I and II inclusions. This film of water would

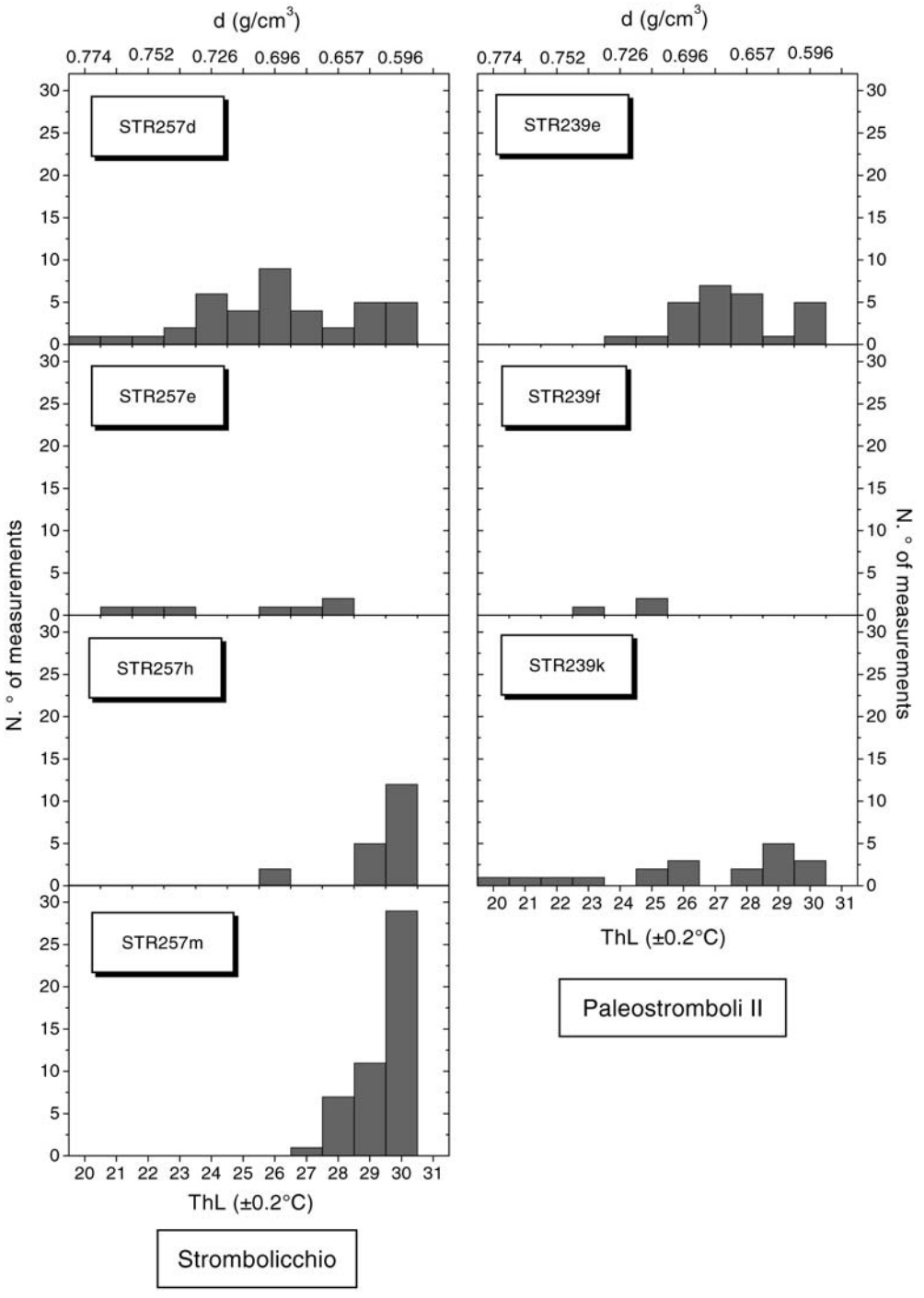

Fig. 5 Homogenisation temperatures in the liquid phase (ThL) for type I CO_2 inclusions in Strombolicchio (*left side*) and Paleostromboli II (*right side*) quartzite nodules (*d* density, *N. of measurements* number of analysed inclusions)

be invisible to microscopic observation because of the inadequate separation capacity of the microscopes. Although this film of water may represent only a small volume (few %) of the total fluid inclusion, neglecting it may produce significant errors in estimates of the composition and density of the fluid inclusions. The maximum amount of water present in type I and II inclusions can be based on the assumption that the maximum volume of liquid water is about 5%. Such a volume should be visible at least in elongated subcylindrical inclusions (see Fig. 5.3 in Bodnar et al. 1985). For type I inclusions with the highest (lowest ThL) and lowest (highest ThL) CO_2 densities, the maximum H_2O contents (calculated in the H_2O–CO_2 system) are 13 and 17 mol% respectively. For the type II inclusions with the maximum and minimum densities, the upper limit of water content is about 24 and 43 mol% respectively.

In summary, the above data confirm that both type I and II contain a CO_2-rich fluid.

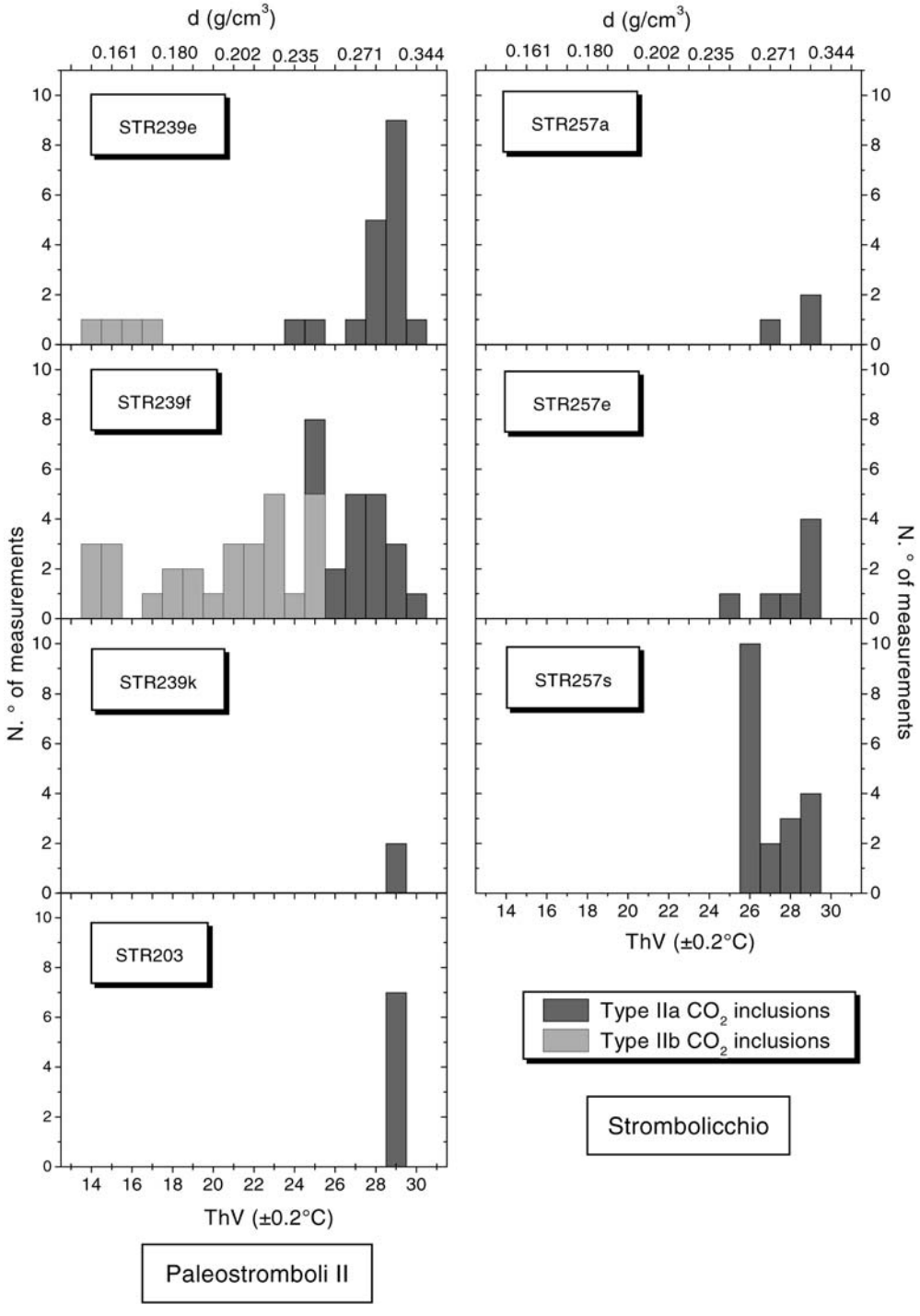

Fig. 6 Homogenisation temperatures in the vapour phase (ThV) for type IIa and IIb CO_2 inclusions in Strombolicchio (*right side*) and Paleostromboli II (*left side*) quartzite nodules (*d* density, *N. of measurements* number of analysed inclusions)

Chemical data of silicate-melt inclusions

Electron microprobe analyses of type IVa silicate-melt inclusions have been performed on three Strombolicchio and two PSTII quartzite nodules (Table 2). Thirteen homogeneous and transparent type IVa inclusions were analysed in quartz crystals from PSTII nodules and seven from Strombolicchio nodules. An average of the bulk composition of the unmixed glass was also obtained on an inhomogeneous type IVb inclusion (PSTII sample), using a 10-μm spot. Interstitial glass was also investigated in sample STR239j from PSTII (Table 3).

Both type IVa and IVb silicate-melt inclusions are rhyolitic in composition (Table 2) but the bulk composition of the inhomogeneous glass (type IVb) is Ca-Fe-enriched and Si-K-depleted with respect to type IVa. Similarly, the interstitial glass, mostly rhyolitic in composition and subordinately dacitic, has lower SiO_2 and Na_2O, and higher FeO, TiO_2, MgO and CaO with respect to most of the type IVa silicate-melt inclusions (Table 3).

Table 2 Representative electron microprobe analyses of type IVa silicate-melt inclusions. An average of the bulk composition of an inhomogeneous type IVb inclusion (PSTII sample) is also reported (*b.d.l.* below detection limit)

Sample	STR203				STR239j	STR257d		STR257m		STR257i	STR257z1	
Type	a	a	a	b	a	a	a	a	a	a	a	a
SiO_2	76.28	75.06	73.51	68.75	76.70	72.83	73.40	75.65	70.21	74.59	74.32	73.86
TiO_2	b.d.l.	0.07	0.04	0.08	b.d.l.	0.20	0.09	0.22	0.26	b.d.l.	b.d.l.	0.42
Al_2O_3	11.24	10.57	12.41	11.34	10.36	13.33	11.38	10.8	12.37	14.26	15.32	14.82
FeO	1.23	0.93	1.11	2.04	0.98	1.09	0.97	1.22	3.84	0.18	0.13	0.37
MnO	0.12	0.12	0.13	0.27	b.d.l.	b.d.l.	b.d.l.	b.d.l.	0.22	b.d.l.	b.d.l.	b.d.l.
MgO	0.10	0.12	0.10	0.14	0.13	b.d.l.	0.08	0.09	0.13	b.d.l.	b.d.l.	b.d.l.
CaO	0.96	0.85	0.77	2.76	2.00	0.18	0.41	0.62	0.57	0.54	1.59	1.24
Na_2O	4.18	4.11	4.46	4.56	2.93	4.99	8.43	4.53	2.27	3.34	2.88	1.91
K_2O	4.39	4.95	4.78	3.70	3.83	6.55	4.62	5.33	6.30	6.86	5.64	5.46
P_2O_5	b.d.l.	b.d.l.	b.d.l.	b.d.l.	b.d.l.	0.12	b.d.l.	b.d.l.	b.d.l.	0.05	b.d.l.	b.d.l.
Cl	0.22	0.04	0.04	0.08	0.14	0.08	0.29	0.32	b.d.l.	0.05	b.d.l.	0.47
Total	98.76	96.84	97.37	93.74	97.07	99.37	99.67	98.78	96.17	99.87	99.88	98.55

Table 3 Electron microprobe analyses of interstitial glasses from Paleostromboli II, STR239j nodule

Analysis	#1	#2	#3	#4	#5	#6
Position[a]	A	B	A	B	B	B
SiO_2	72.97	68.59	73.11	68.06	70.96	72.32
TiO_2	0.55	0.22	0.44	0.74	0.61	0.57
Al_2O_3	11.48	10.33	10.46	12.16	12.06	10.67
FeO	4.04	5.40	4.68	6.42	4.42	3.47
MnO	0.07	0.29	0.09	0.17	0.13	b.d.l.
MgO	0.68	0.33	0.53	1.05	0.86	0.55
CaO	2.27	5.14	2.63	2.99	2.83	1.45
Na_2O	2.81	2.32	2.59	3.25	3.50	2.52
K_2O	4.24	3.81	4.48	3.37	4.24	4.57
P_2O_5	0.11	0.07	0.07	0.13	0.13	0.09
Cl	0.10	0.10	0.14	0.14	0.14	0.11
Total	99.32	96.6	99.22	98.48	99.88	96.32

[a]A, interstitial glass inside the nodule; B, interstitial glass in a reaction corona between the host lava and the quartzite nodule; from #4 to #6, increasing distance from the host lava; b.d.l., below detection limit

In the silicate-melt inclusions, the concentrations of K_2O, Al_2O_3 and Na_2O decrease with increasing silica whereas FeO, TiO_2 and CaO do not seem to be correlated with silica (Fig. 7). MgO content is very low and close to the instrumental detection limit.

The silicate-melt inclusions of Strombolicchio show more scattered compositions, with lower SiO_2 and higher TiO_2, K_2O and Al_2O_3 with respect to the silicate-melt inclusions of PSTII.

In the interstitial glasses, FeO, CaO, TiO_2 and MgO show negative correlations with silica; Na_2O and Al_2O_3 are roughly constant and K_2O is positively correlated with silica.

The positive correlation of K_2O with silica in the interstitial glasses is opposite to that shown by the silicate-melt inclusions. In STR239j, however, the interstitial glass analyses were performed in the reaction corona and at a different distance from the host lava. The glass composition becomes less acid as it moves towards the host rock, indicating interaction processes between the two types of melts.

Discussion

Origin of quartzite nodules

With regard to the origin of the quartzite nodules, some explanation is needed for their presence in most of the Aeolian volcanoes (cf. Francalanci and Santo 1993; Peccerillo et al. 1993; Zanon 2001), although there is no great abundance of quartzite rocks in the crustal basement of the Aeolian Arc (see preceding description of the Aeolian basement).

Quartzite nodules at Stromboli were found only in the calc-alkaline lavas of Strombolicchio and PSTII. Previous studies report the occurrence of felsic nodules in Strombolicchio since the beginning of the 20th century (Johnston-Lavis 1893). Honnorez and Keller (1968) suggest that these felsic nodules have a metamorphic origin by contact of sedimentary rocks with calc-alkaline lavas. Pezzino and Scribano (1989) describe two types of quartzite nodules: the first is of sedimentary origin from quartzite and the second of metamorphic origin from the Hercynian Calabro-Peloritano basement.

Quartzite nodules are also described by Francalanci and Santo (1993), Peccerillo et al. (1993) and Zanon (2001), as occurring on the Filicudi, Alicudi and Vulcano islands respectively. Francalanci and Santo (1993) describe equigranular metamorphic xenoliths made up of quartz, K-feldspar, plagioclase and thin glass films. Peccerillo et al. (1993) describe quartzitic and quartz+pyroxene nodules with equigranular granoblastic texture. Triple points and interstitial hypocrystalline/microcrystalline films are also present. An origin from the melting of quartz granules and Al-bearing phases is assumed. Zanon (2001) describes quartz-rich xenoliths with two quartz types and suggests their restitic origin from a metamorphic quartz-rich rock underlying the Aeolian archipelago.

The quartzite nodules from both Strombolicchio and PSTII are mainly made up of quartz crystals with subordinate and resorbed K-feldspar and plagioclase, together with interstitial minerals and glasses. Three

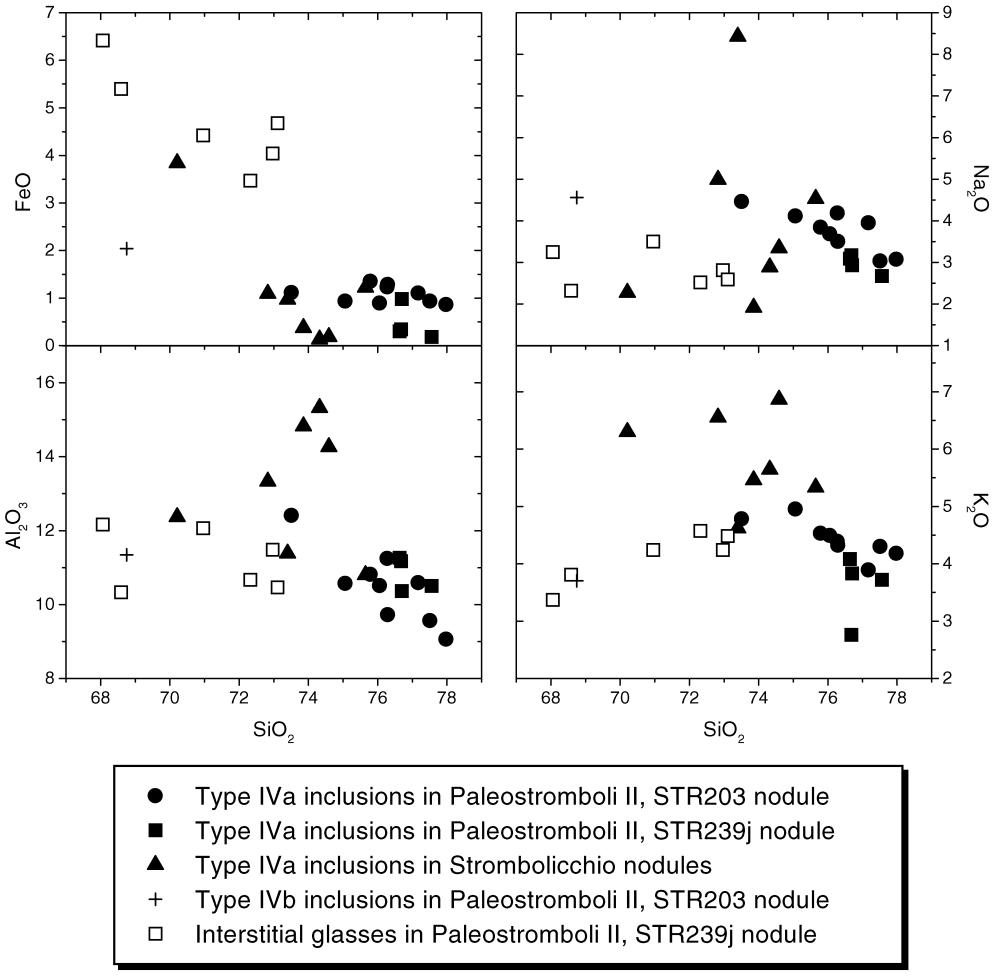

Fig. 7 Variation diagrams of major elements (wt%) for type IV silicate-melt inclusions and interstitial glasses

different quartzite nodules have been identified on the basis of textural features. Their petrographic characteristics suggest that these different types of quartzite xenoliths represent restitic rocks produced by the partial melting of a crustal rock. The nearly exclusive presence of quartz is, in fact, interpreted as the result of the melting process, where the quartz remains as residual phase. Also the observed accessory minerals may represent residual phases whereas the interstitial minerals, generally small, do not show evidence of re-absorption processes and seem to be crystallised by a final magmatic liquid.

Textural evidence indicates that the quartz grains represented by RQ and LRQ are new quartz crystals replacing ReQ crystals. This, and the polygonal granoblastic textures with definite triple points of RQ and LRQ, suggests that these types of quartz are the result of quartz static re-crystallisation during thermal metamorphism. The occurrence of primary type IV melt inclusions in RQ and LRQ grains indicates that quartz types grow in the presence of a silicate acidic melt. Thus, static re-crystallisation developed, at least in part, after partial melting had already occurred. The final result of restitic quartz annealing is the formation of polygonal granoblastic textures with definite triple points.

Since the degree of static re-crystallisation (and of the grain sizes) depends on temperature, the observed textures, i.e. the development of small/medium inequigranular and large equigranular polygonal granoblastic nodules, may be interpreted as the result of differences in temperature which produce a different rate of re-crystallisation. In particular, the disappearance in sequence of ReQ and LRQ quartz suggests a progressive increase in temperature and re-crystallisation rate. This thermal gradient may develop in proximity to a magma rest at the magma/wall rock contact.

Finally, the formation of break-up nodules, i.e. of resorbed ReQ and RQ+LRQ aggregates, possibly occurred during a later stage of partial melting, following a temperature increase. This may occur when restitic quartzite of wall rock is included in magma as nodules for a relatively long rest period.

There are few constraints allowing us to identify the source crustal rocks of the xenoliths. The undulose extinction of ReQ quartz may be indicative of its metamorphic nature, whereas the large amount of residual quartz is evidence of its sialic composition. This is also confirmed by the acidic composition of the melt inclusions and interstitial glasses.

The negative correlations of silica with Al_2O_3, K_2O and Na_2O in the silicate-melt inclusions could be explained by K-feldspar and plagioclase post-entrapment crystallisation, but no daughter minerals were found in the melt inclusions analysed. The same trends could be attributed to quartz crystallisation, but no evidence was observed of host mineral crystallisation around the cavity wall of the analysed inclusions. The latter process should also have determined an increase of all major-element contents with the decrease in silica.

By contrast, non-modal partial melting of a rock consisting mainly of quartz, K-feldspar and plagioclase could explain the negative correlations of K_2O, Al_2O_3 and Na_2O with SiO_2. The higher K_2O, Al_2O_3 and TiO_2 and lower SiO_2 contents of the Strombolicchio melt inclusions with respect to the PSTII inclusions lead us to hypothesise a significant presence of other mineral phases, such as biotite and muscovite, in the source rock of the Strombolicchio quartzite nodules. Furthermore, the higher FeO and CaO and the lower silica contents of type IVb silicate-melt inclusions suggest the presence of Fe-Ca-bearing minerals in the source rock of PSTII nodules. The different compositions of the silicate-melt inclusions, even in the same xenolith, clearly indicate a disequilibrium, partial melting of the source rock. In this case, each glass composition is in equilibrium with only a circumscribed portion of the source rock, being affected by the relative proportions of melted local minerals.

As regards the interstitial glasses, they have lower SiO_2 and higher FeO, TiO_2 and MgO contents; the correlations of the latter elements with silica and potassium, moreover, are negative. These chemical characteristics have to be interpreted not only in terms of disequilibrium partial melting processes but also by considering the presence in the glass of quenching minerals mainly constituted by quartz, and interaction with the host magma. Indeed, the silica and potassium contents decrease in the glass composition, and TiO_2, MgO, FeO and CaO increase moving towards the host rock, suggesting that the interstitial glass compositions were affected by interaction with the host magma, which is far less evolved (calc-alkaline basaltic andesite). The quenching crystallisation of quartz also leads to a decrease in silica and an increase in the contents of the other elements. The compositions of the interstitial glasses, therefore, derive from a combination of three different processes.

Considering the foregoing evidence, it is reasonable to assume as source rocks of the quartzite nodules the sialic metamorphic rocks coming from the crustal basement and made up of quartz, K-feldspar and plagioclase, with a lower amount of biotite and muscovite and/or general Ca–Fe minerals. As the continental crust below the Aeolian Arc is considered to belong to the Calabride domain, the source rocks may be represented by felsic granulites or granitic gneiss.

Partial melting of these rocks can be described by the albite–orthoclase–quartz ternary diagram (Fig. 8). Here, the granitic minimum of temperature becomes a ternary

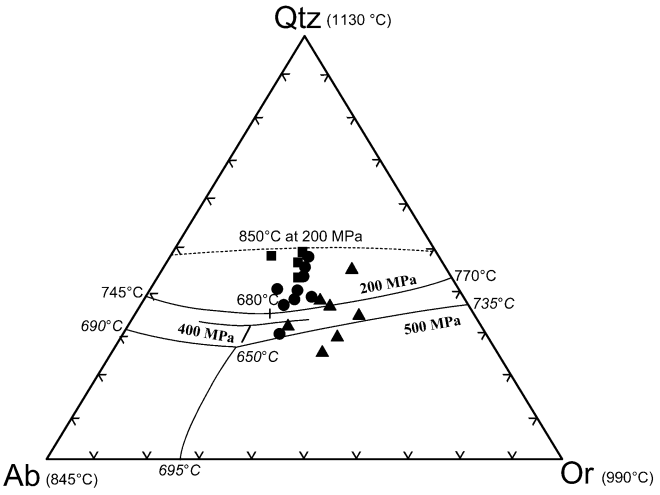

Fig. 8 Ternary quartz (Qtz)–albite (Ab)–orthoclase (Or) diagram after Winkler (1978), from Tuttle and Bowen (1958) and Shaw (1963). *Symbols* are as in Fig. 7

eutectic at around PH_2O>400 MPa (Tuttle and Bowen 1958; Luth et al. 1964). Ranging from PH_2O=200 to 500 MPa, the minimum temperature changes from about 700 to 660 °C. Partial melting of the nodule source rocks is, therefore, able to occur during contact with calc-alkaline magmas, which have a basic composition and consequently a higher temperature. The estimated temperature of the calc-alkaline basaltic andesite magmas, obtained in previous studies on clinopyroxene-hosted silicate-melt inclusions, is around 1,220–1,250 °C (Vaggelli 1992, 1993).

Melting starts at the eutectic point where quartz, K-feldspar and plagioclase coexist. The first phase to disappear at the eutectic point has to be K-feldspar or plagioclase, as quartz is still abundant and remains as residual phase. The compositions of Strombolicchio and PSTII silicate-melt inclusions plot in distinct fields in the ternary diagram of Fig. 8. PSTII inclusions, in particular, plot at the same distance from albite and orthoclase and define a rough alignment towards quartz. This seems to indicate that melt composition has already left the cotectic line and moves in the quartz field. Strombolicchio melt inclusions are shifted toward orthoclase, due to their higher K_2O contents which probably derived from a more important role played by biotite and muscovite in the source rock. Their trend is not well defined, owing to a complete disequilibrium during melting, and also because the analyses came from four separate nodules. All the melt-inclusion compositions, however, approach the 850 °C isotherm at PH_2O of 200 MPa (Tuttle and Bowen 1958). Thus, it is reasonable to expect temperatures from that one of the granite eutectic up to about 850–900 °C for these acid melts.

CO_2 origin

The CO_2-rich fluid inclusions were found only in quartz grains and none were detected in the phenocrysts of the host lavas. A previous systematic investigation of the presence of fluid inclusions in Stromboli rocks from different petrological affinities has revealed the absence or paucity of free fluids during magma crystallisation, as no CO_2 and/or H_2O inclusions were found. In addition, neither the microthermometric investigation nor the Raman analyses on the shrinkage bubbles of the silicate-melt inclusions in phenocrysts have ever shown the presence of CO_2 or other gases (Vaggelli 1992; Vaggelli et al. 1993). Since Strombolian magmas are poor in CO_2, the CO_2 of both type I and II inclusions in quartzite nodules is therefore assumed to derive from the crustal basement and not from the host magma.

The CO_2 in the fluid phase may have originated from de-carbonatisation of marble, commonly present as lenses in the Calabrian crustal section, or from oxidation of graphite, a common constituent of metapelites of Calabria. However, no traces of marble nor of thermometamorphic minerals such as wollastonite have been found in the petrographic observations of the nodules. We are therefore unable to invoke a CO_2 origin from metacarbonates, nor from graphitic levels.

The last possible hypothesis for the origin of the CO_2 is related to the presence of CO_2-rich and/or H_2O±NaCl+-CO_2-rich fluid inclusions in the source rocks. These fluids could be released from the fluid inclusions during partial melting or as a consequence of decrepitation phenomena during heating processes. If the released fluid were only a CO_2-rich fluid, then this process alone could explain the trapping of CO_2 in the studied inclusions. If the released fluid was a H_2O±NaCl+CO_2 fluid, immiscibility phenomena may have produced CO_2-rich and H_2O±NaCl-rich fluids. In particular, the immiscibility process and the occurrence of isolated type I inclusions in RQ+LRQ quartz are in agreement with the experimental data of Gibert el al. (1998). These authors have shown that fluid immiscibility in the H_2O+NaCl+CO_2 system is particularly favoured at a pressure≤400 MPa and temperature≥700 °C. Pressure–temperature values during type I inclusion trapping (see below) are compatible with these conditions. During quartz re-crystallisation (and the trapping of primary type I inclusions), two immiscible fluids (a CO_2-rich and a H_2O±NaCl-rich fluid) may therefore have been present. The different wetting behaviour of the CO_2-rich and aqueous fluids may result in the selective trapping of the CO_2-rich fluid and escape of the aqueous fluid (Gibert et al. 1998). Indeed, aqueous fluids have a low wetting angle, so a complete interconnectivity of pores is achieved and these fluids are able to leave the system (Watson and Brenan 1987) and eventually dissolve into the melt. On the contrary, CO_2-rich fluids have a high wetting angle which precludes widespread interconnectivity of porosities. Consequently, CO_2 remains in the system in isolated pores at the grain corners and is then trapped in isolated (type I) fluid inclusions during thermal re-crystallisation of RQ+LRQ quartz.

An in-situ origin for the CO_2 is compatible with the composition of the fluid inclusions which are expected to be originally present in the source rocks of the quarzite nodules. Indeed, these rocks are assumed to be sialic metamorphic rocks, coming from the Calabrian crustal basement. In general, medium- to high-grade metamorphic rocks, such as those constituting part of the Calabrian basement, contain CO_2-bearing fluid inclusions (Roedder 1984). The presence of both CO_2-rich and H_2O-CO_2-rich inclusions in the rocks of the Calabrian basement is also confirmed by Herms and Schenk (1992) who found these types of fluid inclusion in metapelites under granulite-facies conditions in the Serre Massif.

Evidence of fluid-inclusion re-equilibration

The textural characteristics (i.e. decrepitation features) shown by many medium to large and some small type I inclusions in all samples, except for STR257m, clearly indicate that they were affected by re-equilibration processes. Decrepitation textures develop when the difference between the internal pressure and external pressure of fluid inclusions is so high as to cause the brittle deformation of the host minerals.

The decrepitation features observed in the studied inclusions are similar to the re-equilibration textures of aqueous, synthetic fluid inclusions in quartz subjected to internal overpressure, found in an experimental study by Vityk and Bodnar (1995). Overpressure within fluid inclusions can be caused either by isobaric heating or isothermal decompression of the host crystals. Vityk and Bodnar (1995) found decrepitation texture only occasionally in fluid inclusions subjected to isobaric heating to 700 °C, whereas brittle deformation characterises many medium- to large-sized (>10 μm) inclusions subjected to decompression with relatively small temperature variation (from 700 to 600 °C). The different behaviour of fluid inclusions subjected to re-equilibration depends on several factors: (1) the final P–T condition of re-equilibration; (2) the P–T path followed by the inclusions during re-equilibration; and (3) the effective pressure application rate (loading rate) during re-equilibration (Vityk and Bodnar 1995). In particular, low temperature and rapid loading rate facilitated the brittle deformation of fluid inclusions whereas under high temperature and low loading rate conditions, the inclusions re-equilibrate plastically (i.e. the inclusions are affected by stretching and/or diffusion processes).

Other features of the type I inclusions, with the exception of sample STR257m, which can be related to a re-equilibration process are (1) the wide range of Th (i.e. densities); (2) the positive correlation between fluid-inclusion size and Th; and (3) the multimodal shape of the Th histograms shown by some samples (STR257d, STR239e and STR239k). All these characteristics were observed by Vityk and Bodnar (1998) in aqueous,

synthetic fluid inclusions subjected to rapid and nearly isothermal decompression (fast loading rate). Some samples (STR257e and STR239f) do not show the multimodal shape of the Th histogram even though the type I inclusions display decrepitation features. Type I inclusions are rare in such samples, however, and there are too few data available for an evaluation of the histogram shapes.

The wide range of Th (density) can be explained by the different degree of equilibration. Some inclusions may preserve the original (high) density, others may be totally re-equilibrated to the new P–T condition and show the lowest densities, and yet others underwent partial decrepitation (i.e. formation of fractures around the inclusions without fluid loss), or partial leaking or stretching to produce intermediate densities.

The positive correlation between inclusion size and Th shown by inclusions subjected to instantaneous decompression can be attributed to different deformation mechanisms between large and small inclusions (Vityk and Bodnar 1998). The former deformed in brittle fashion, immediately after they were subjected to overpressure and therefore always show a decrease in their original density. Smaller inclusions deformed preferentially by a slow plastic flow mechanism, allowing them to maintain internal overpressure (and therefore higher density) for a longer time.

Origin of CO_2 inclusions

Type I

Type I CO_2 inclusions formed during RQ and LRQ quartz re-crystallisation are primary in origin. As already shown, quartz re-crystallisation developed as a consequence of a thermal gradient in proximity to a magma rest at the magma/wall rock contact. After their formation and incorporation within the ascending magma, the nodules underwent decompression and heating, with the consequence that type I inclusions were subjected to high internal overpressure. This process caused partial decrepitation of many large and some small inclusions hosted in both equigranular and inequigranular nodules (samples STR257d, STR257e, STR257h, STR239e, STR239f and STR239k). Since brittle deformation is facilitated by lower temperature and rapid pressure variations, decrepitation processes probably occurred in response to fast decompression during magma ascent and before the definitive thermal re-equilibration of the nodules at the temperature of the host magma.

After decompression and thermal heating, some decrepitated primary inclusions were not re-healed and completely lost their CO_2-rich fluid, producing the open, dark inclusions frequently observed in RQ and LRQ quartz. Some of the released fluids were trapped again in the secondary type II inclusions (see below) at the new P–T conditions reached by the nodules.

The type I inclusions in sample STR257m do not show clear re-equilibration textures (brittle deformation), so they may record the original density of the CO_2-rich fluid. However, since this nodule, along with the others, underwent heating and decompression after its formation, the primary type I inclusions were also subjected to overpressure, and re-equilibration processes can therefore also be invoked for these inclusions. If these inclusions were also subjected to re-equilibration, the absence of brittle textures indicates that the fluid inclusion deformed plastically. Therefore, sample STR257m followed a different history from that of the other xenoliths. The abundance of MQ grains in this sample can be related to a relatively long permanence within the host magma, which suggests that nodule STR257m was included early in the host magma and may have reached thermal equilibrium with the magma before the ascent of the latter. In this case, fluid-inclusion re-equilibration can be related to a slow heating up to the magma temperature which triggers the plastic deformation of fluid inclusions. After heating, this nodule also underwent an upwelling, with the result that some of the type I inclusions totally decrepitated and formed the dark inclusions which can also be observed in the RQ quartz.

Type II

These are distributed along intra-crystalline fractures which clearly denote a secondary origin. A pseudosecondary origin may also be invoked for some type IIa inclusions in Strombolicchio samples, as the trails stop before the crystal rims, in correspondence to the development of type III inclusions which form later than type IIa.

In general, the microfracturing of nodule crystals, which produces trails of secondary/pseudosecondary type II fluid inclusions, can be considered to have formed in response to decompression and thermal stresses during magma migration towards the surface. Type II inclusions were therefore trapped after decompression and thermal re-equilibration to the magma temperature of the nodules. The CO_2-rich fluid trapped in type II inclusions can be released from the decrepitated type I inclusions. This fluid penetrated the microfractures and was trapped after healing.

Although most of the type II inclusions represent the trapping of only a CO_2-rich fluid, a consistent minority of type IVa inclusions associated with type IIa represents the trapping of two immiscible fluids—silicate melt and CO_2-rich fluid. For the associated type IIa and IVa inclusions, we have to invoke a cogenetic origin. Refilling of quartz fractures and cracks with type IIa/type IVa inclusions therefore occurred after the source rock melting.

The moderate density variation shown by type IIa inclusions suggests that these inclusions were trapped at relatively constant P–T conditions, and probably during a rest of the magma in a reservoir.

Type IIb CO_2-rich fluid inclusions are observed only in PSTII samples, and are not associated with glass inclusions. Textural relationships indicate that type IIb inclusions were trapped later than type IIa. This late nature and their relatively low ThV suggest that type IIb were trapped at very low pressure during the final upwelling of the magma towards the surface.

Type III

These inclusions are not suitable for microthermometric investigations because of the very low density of the entrapped fluid (CO_2?). However, the clear distribution along inner rims of quartz crystal in Strombolicchio samples suggests a "primary" origin with respect to a final crystallisation process during magmatic conditions.

Trapping pressure

Isochores for selected fluid densities (Figs. 9, 10 and 11), calculated by the method described by Kerrick and Jacobs (1981) and assuming a pure CO_2 system, are shown in Figs. 9 and 11 for type I and II inclusions respectively. The trapping pressure of the fluid inclusions can be calculated from the isochores if the trapping temperature is known.

The trapping temperatures of type I inclusions must be at least those of the granite eutectic as these inclusions were trapped during RQ and LRQ crystal growth in the presence of a silicate acidic melt. Since type I inclusions were subjected to re-equilibration as a consequence of internal overpressure, most or all of their original densities may have been modified (decreased) during this process. Assuming that the maximum density of type I inclusions (corresponding to ThL=20 °C) is still representative of the inclusion density before re-equilibration, from the intersection of the granite eutectic and the isochore of ThL=20 °C we can calculate a minimum pressure of 290 MPa for the formation of type I inclusions (Fig. 9).

Information on the formation pressure of type I inclusions can also be derived from the re-equilibrated type I inclusions present in sample STR257m. As shown above, the STR257m sample reflects a different P–T evolution with respect to the other nodules, as suggested by the presence of MQ grains and the absence of type II inclusions and of ReQ grains. For this sample, inclusion re-equilibration was related to a slow heating process to the temperature of magma (1,250 °C) as a consequence of the incorporation and long rest of the nodule within the host magma.

Assuming that the fluid inclusions re-equilibrated at the temperature of magma, the re-equilibration pressure (around 290 MPa) can be calculated from the isochore of the minimum fluid density (ThL=30.5 °C; Fig. 9). This pressure notably coincides with the minimum trapping pressure for the formation of type I inclusions. A possible

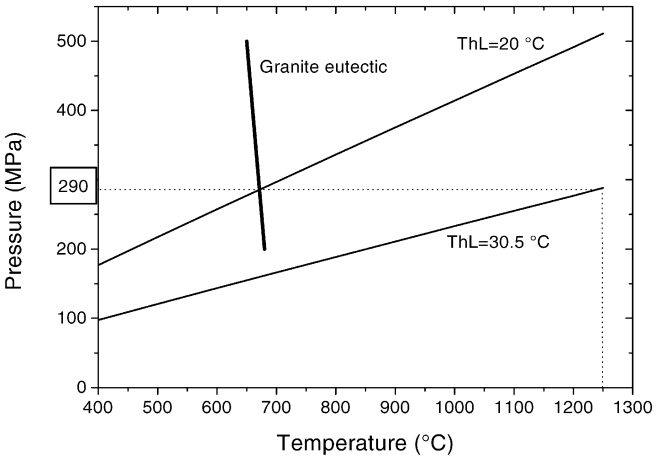

Fig. 9 P–T binary diagram with isochores at ThL=20 and 30.5 °C. The variation of granite eutectic is also reported. *ThL* Homogenisation temperature in the liquid phase

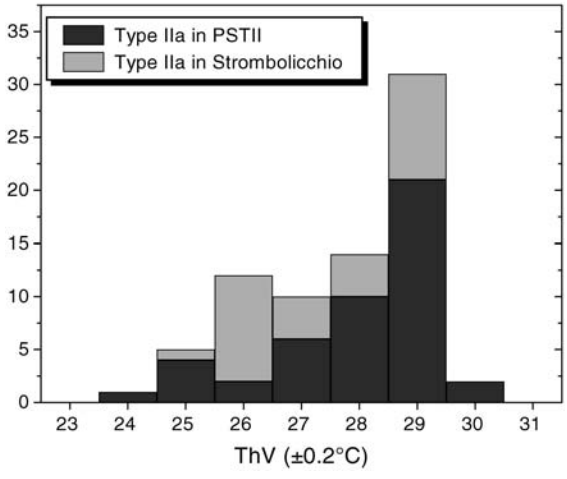

Fig. 10 Homogenisation temperatures in the vapour phase (ThV) for type IIa CO_2 inclusions in Strombolicchio and Paleostromboli II quartzite nodules

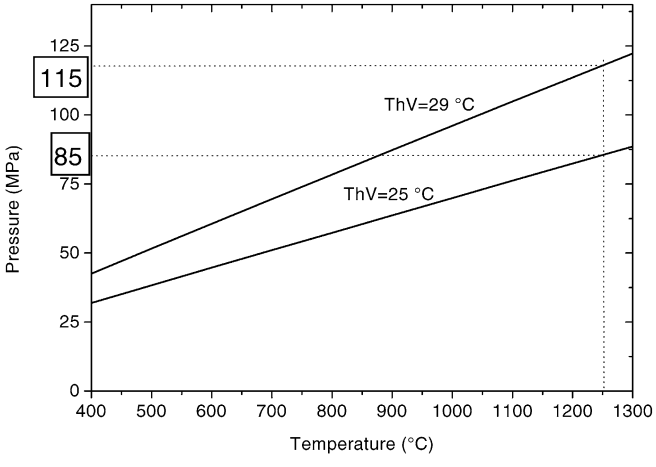

Fig. 11 P–T binary diagram with isochores at ThV=25 and 29 °C. *ThV* Homogenisation temperature in the vapour phase

interpretation of this similarity is the following: (1) the type I inclusions were effectively trapped at 290 MPa; (2) the type I inclusions showing the lowest density, in STR257m, represent inclusions which have fully re-equilibrated as a consequence of isobaric heating (up to a temperature close to 1,250 °C) at the site of a magma rest.

As shown above, type IIa inclusions record the P–T conditions after decompression and heating (up to the magma temperature) of the nodules. The moderate density variation shown by this inclusion type suggests that they were trapped at relatively constant P–T conditions, possibly during a rest of the magma in a reservoir. The isochoric relation for the most common fluid density (ThL=25–29 °C; Fig. 10) and magma temperature (1,250 °C) gives a narrow range of pressures between 85 and 115 MPa for this magma rest (Fig. 11). This agrees with pressure data found by Vaggelli et al. (1991, 1993) who describe the presence of a few CO_2 inclusions with comparable ThV in an olivine microphenocryst from a calc-alkaline lava.

The second fracturing and CO_2-rich fluid trapping event is recorded by the type IIb inclusions. The late trapping nature of these inclusions and their relatively low density (ThV) suggest that type IIb were formed at very low pressure (depth), probably during the final upwelling of the magma towards the surface. This final stage is assumed to have stopped near the surface, with the appearance of type V aqueous inclusions. The latter are both vapour- and liquid-rich aqueous inclusions, presumably representing post/syn–eruptive boiling conditions.

All the calculated pressures have been derived assuming a CO_2 pure system. However, because of the possible presence of an invisible, thin water film (<5% in volume) within the inclusions, type I and II inclusions may contain a significant concentration of water. Neglecting this could lead to errors in isochore calculations, and hence in pressure estimates. An attempt was made to determine the maximum error in pressure evaluation by assuming that the highest volume of H_2O in the studied inclusions is 5%. Using this value, the compositions, densities and isochores (calculated according to Kerrick and Jacobs 1981) of the most significant inclusions have been computed in the H_2O–CO_2 system. From the isochore of the type I inclusions with maximum density, we obtained a higher trapping pressure value (about 310 MPa) than for the pure CO_2 system. Following the same procedure, pressures between 160 and 130 MPa were obtained for the trapping of type IIa inclusions with the most representative densities. Such an error would produce a relatively small variation in the depth evaluation of the first magma rest, and a larger difference in the estimated depth of the shallow magma chamber.

Conclusions and volcanological implications

Among the Stromboli rocks, quartzite nodules are found in Strombolicchio (about 200 ka) and PSTII (about 60 ka) calc-alkaline lavas. They have been interpreted as restites

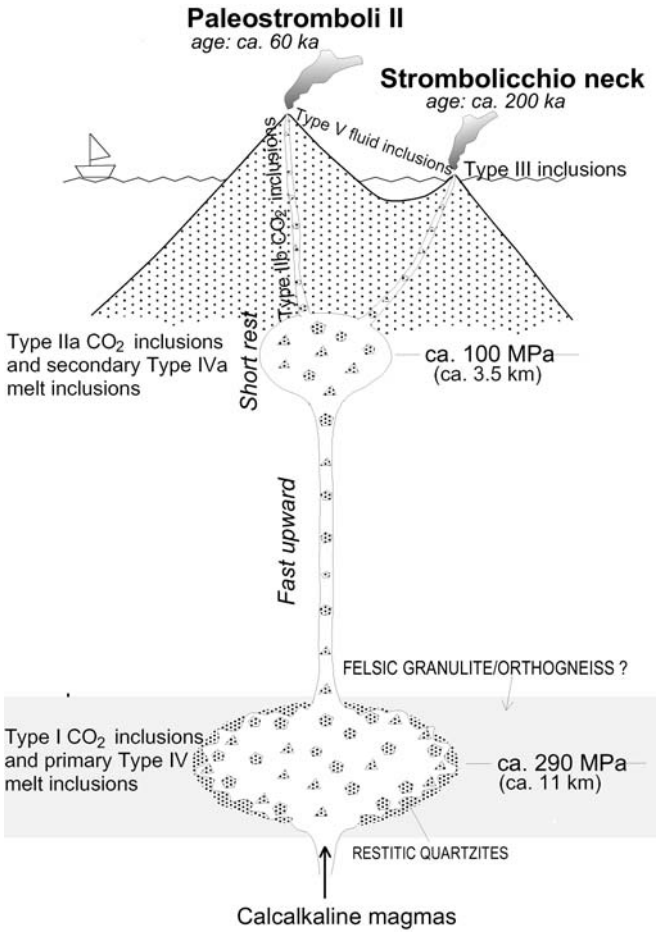

Fig. 12 Sketch of the volcanic plumbing system during the emplacement of both Strombolicchio and PSTII calc-alkaline lavas. In the deep magmatic reservoir, the wall-rock partial melting process and the restitic quartz re-crystallisation occur at different temperatures

which formed after a partial melting process at varying degrees and involving felsic crustal rocks, and occurring at the magma/wall rock contact. Restitic quartz underwent re-crystallisation at relatively high temperatures, and the different petrographic textures of the studied nodules are interpreted as being due to temperature differences of quartz re-crystallisation.

The quartz grains contain five types of fluid inclusion. Textural and microthermometric investigations on type I CO_2-rich inclusions, and the combination of different and significant temperatures and isochores give a pressure value of about 290 MPa (Fig. 9). If the pressure regime regulating the trapping environment of type I inclusions is assumed to be lithostatic, and using an average density value of 2.7 g/cm^3 for the crustal layer section below Stromboli (Barberi et al. 1994), the type I inclusions register a depth of around 11 km. The presence of a magmatic reservoir is assumed at this depth for both the Strombolicchio and PSTII calc-alkaline magmas (Fig. 12). Several processes seem to occur here: (1) source rock partial melting with formation of restitic quartzites where

quartz re-crystallises at least at the temperature of the granitic eutectic; (2) trapping of type I CO_2-rich inclusions and primary type IV silicate-melt inclusions during quartz re-crystallisation; (3) pull-out of the nodules; and (4) rest and break-up by isobaric heating of some nodules (i.e. STR257m; Fig. 12). The pull-out of the restitic quartzites from the magma chamber walls and their ascent allow them to preserve the textures of equigranular and inequigranular nodules. A longer rest at this depth in the magma chamber is, on the other hand, responsible for the formation of break-up nodules.

Textural and microthermometric studies on type IIa CO_2-rich inclusions provide a mean trapping pressure of about 100±15 MPa, corresponding to a depth of about 3.5 km where a shallow magma chamber should have been present during the outpouring of both the Strombolicchio and PSTII calc-alkaline magmas (Fig. 12). This depth corresponds more or less to the transition to the crustal basement, where a lithological discontinuity is expected. The type IIa inclusions and type IVa silicate-melt inclusions of secondary origin were generated at this magma rest. Type IIb CO_2-rich inclusions were formed during ascent of the nodules from this depth to the surface.

The formation of type III inclusions, with final crystallisation of quartz as limpid coronas, is assumed to have occurred at very shallow depth (probably at the surface) only in the Strombolicchio nodules. The interstitial acidic melt can crystallise either as quartz limpid coronas when nodule cooling is slow (as probably occurred in the central part of the Strombolicchio neck), or as glass and cristobalite microcrystals when nodule cooling is fast.

Several volcanological and petrological implications arise from the results presented above. The nodules must have undergone a fast upward movement in order to explain the brittle behaviour of many type I inclusions. Slow decompression would have produced a plastic deformation of re-equilibrated fluid inclusions and would not show brittle textures (Vityk and Bodnar 1995). A short rest in the shallower magma reservoir is also supposed, as most type I inclusions are not completely re-equilibrated. This is also corroborated by the fairly primitive composition of the host magmas (basaltic andesites with average of MgO=6.5%, Cr=200 ppm and Co=34 ppm; Francalanci et al. 1989, 1993; Hornig-Kjarsgaard et al. 1993), indicating a reduced role of the evolutionary processes. Furthermore, a faster upward movement from the shallower reservoir to the surface is hypothesised for the Strombolicchio than for the PSTII magmas, in order to prevent the formation of type IIb inclusions.

As the quartzite nodules are interpreted to be the restitic product of a partial melting process involving felsic metamorphic rocks surrounding the deepest magmatic reservoir, crustal rocks such as "felsic granulites/orthogneiss" are assumed to be present below Stromboli at a depth of around 11 km.

On the basis of melt-inclusion data, a source rock with a more significant biotite and muscovite content has been hypothesised for Strombolicchio than for the PSTII xenoliths, which means that, at the same depth but at a different time, partial melting affected portions of source rocks with slightly different mineralogical composition. Metamorphic rocks are usually heterogeneous at a small scale, and the process may be imagined as an enlargement or a small lateral shift of the magma chamber.

The fact that the Stromboli magmas led to the formation of restitic quartzites has significant implications with regard to magma evolution processes because it is direct evidence of crustal contamination. Interstitial glass compositions in STR239j nodules have indicated an interaction of host magma with glass of a nodule corona (Table 3). The acidic melts derived from the first degrees of partial melting of the source rocks are, however, no longer present in the crustal nodules where only small amounts of interstitial glass can be found. They have thus interacted in some way with magmas present in the reservoir, which to some extent changed their chemical and isotope compositions.

The presence of quartzite nodules only in the calc-alkaline rocks of significantly different ages can be explained in several ways, but only one of these is plausible. It could be hypothesised that the calc-alkaline magmas assimilated crustal rocks, leading to the formation of quartzites, and remained in the same reservoirs from 200 to 60 ka without changing their composition. Thus, the more evolved, high-K calc-alkaline magmas, erupted at around 100 ka (PST I), were derived from a third magma chamber. Alternatively, it may be hypothesised that all the magmas acted in the same two reservoirs but only the calc-alkaline magmas were able to assimilate crustal rocks. According to the following, however, neither hypothesis seems to be plausible: (1) despite the difference in age, the calc-alkaline magmas are always basaltic andesites, with a constant and quite primitive composition which is difficult to maintain for 140×10^3 years; (2) the calc-alkaline magmas show the lowest Sr isotope ratios of Stromboli (Francalanci et al. 1988), so it is difficult to believe that only these magmas assimilated crustal rocks; (3) the calc-alkaline magmas seem to have quite high temperatures which are, however, comparable to those of other Stromboli lavas (Vaggelli, 1992); and (4) apart from submerged rocks, it is evident that high-K calc-alkaline rocks (PST I), more evolved (high-K andesites) and with higher Sr isotope ratios, were erupted between the two calc-alkaline events. Volcanological, stratigraphical and chemical evidence has shown that the calc-alkaline magmas of the PSTII entered the reservoir of high-K andesites of PST I (Francalanci et al. 1988, 1989, 1993), indicating their interaction in the same magma chamber and again invalidating the first hypothesis.

Accordingly, it seems more reasonable to suppose that from 200 to 60 ka, all Stromboli magmas rested at the same depths of about 11 and 3.5 km, and that only the calc-alkaline magmas were able to carry quartzite nodules

to the surface. The latter property may be linked to the particular density of these magmas or, as is more likely, to their short residence time in the reservoirs and/or fast upwelling. The calc-alkaline magmas have in fact a constant, quite primitive composition, which leads us to hypothesise a rather brief transit through the continental crust. Fast upwelling has also been suggested on the basis of fluid-inclusion evidence in quartzite nodules. It can, therefore, be hypothesised that in the presence of a longer magma residence time, xenoliths can be completely digested by assimilitation+fractional crystallisation. These processes lead to increasing potassium and incompatible trace-element contents, silica abundances and Sr isotope ratios of the host magmas, thus generating more evolved and Sr radiogenic magmas with a different serial affinity (high-K andesites of PST I, for example). If this is the case, the main quartzite-forming crustal assimilation processes probably occurred in magmas with different compositions and ages from the calc-alkaline ones. The variable magma residence time in the continental crust at different ages could be linked to variations in the tectonic stress of the area.

Quartzite nodules are also found in other volcanoes of the Aeolian Arc (e.g. Filicudi, Alicudi, Salina and Vulcano), where they seem to have a similar origin (Francalanci and Santo 1993; Peccerillo et al. 1993; Zanon 2001; Frezzotti et al. 2002). This fact indicates that crustal contamination is a common process occurring in most of the other volcanoes of the Aeolian Arc. It can be responsible for a typical characteristic of the Aeolian magmas, which is the steeper evolutionary trends of the magmatic series, crossing the border lines between different fields in the K_2O silica classification diagram (Francalanci 1997 and reference therein). On the basis of mineralogical, chemical and isotope data, crustal contamination processes have also been repeatedly invoked to explain the specific evolutionary trends of the Lipari, Vulcano, Alicudi and Filicudi volcanoes (Barker 1987; Esperanca et al. 1992; Peccerillo et al. 1993; Francalanci and Santo 1993; De Astis et al. 1997). Their polybaric evolution is another common characteristic of the Aeolian volcanoes (e.g. De Astis et al. 1997; Zanon 2001; Frezzotti et al. 2002). Based on fluid-inclusion studies in quartzite nodules, two rest pressures have been found for Vulcano, Salina, Filicudi and Alicudi magmas (Zanon 2001; Frezzotti et al. 2002); these pressure values also include those found at Stromboli. The lowest rest pressure is around 20–100 MPa whereas the highest varies from island to island, ranging between 300 and 600 MPa.

The general evolution of Stromboli, therefore, involves processes which occur in the other volcanoes of the Aeolian Arc, which are similarly characterised by a number of compositional variations of rocks occurring in a short period of time. The presence in the basement of felsic metamorphic rocks affected by partial melting processes also seems to be an evidence that can be extended to the rest of the Aeolian Arc.

The results obtained on Stromboli confirm and better constrain the hypothesis, based on chemical and petrological data, of the existence of two magma chambers at different depths within the crust (Francalanci et al. 1989, 1993). It has been proposed that the deeper reservoir was affected by refilling+tapping+fractionation+assimilation (RTFA) processes, whereas in the shallower magma chamber it is likely that only crystal fractionation occurred. In addition, the calc-alkaline magmas were assumed to have been affected only by a slight fractionation during their ascent to the surface, without undergoing RTFA processes, which conversely affected the evolution of the other Stromboli magmas (Francalanci et al. 1989, 1993).

Recognition of the polybaric evolution of the Stromboli magmas also represents an important contribution to our understanding of the magma evolution and emplacement system. Crystallisation and crustal assimilation processes occurring in the deepest reservoir cause magmas to assume more evolved and volatile-rich compositions. Rapid ascent of these magmas and their entry into the shallower reservoir may have triggered eruption.

The last and most significant observation arising from these results concerns the present-day volcanic system. If the Stromboli plumbing system has remained in a steady-state for such a long time (from 200 to 60 ky), there is no reason to believe that a similar polybaric evolution is not still under way in the current volcanic system. The deepest reservoir may be the place where the magma recharging the shallower system (erupted as pumice) undergoes its evolution and volatile enrichment processes. The fast ascent and injection of this magma into the shallower reservoir (containing the magma erupted as scoriae by "normal" activity) may be responsible for the more violent explosions of the present-day activity.

Acknowledgement Special thanks are due to H.E Belkin who performed the first set of electron microprobe and microthermometric analyses at the USGS in Reston, VA (USA). G.V. is grateful to H.E. Belkin and M.L. Frezzotti for their hospitality, stimulating discussions and advice during her stay at the USGS and at the Vrije Universiteit in Amsterdam respectively. The authors would also like to thank F. Olmi and S. Tommasini for their help during sampling, E.J. Burke for the Raman microprobe analyses, F. Olmi for his valuable support during the microprobe analyses, and A. Borghi, S. Conticelli, C. Maineri and M. Benvenuti for their constructive discussions and suggestions. Gilles Chazot and an anonymous referee are thanked for their useful comments. Dickson M.H. is also thanked. The work was financially supported by the Gruppo Nazionale di Vulcanologia through the Istituto Nazionale di Geofisica e Vulcanologia, by the Dipartimento di Scienze della Terra of Florence (ex 60% funds), and by the CNR Istituto di Geoscienze e Georisorse Florence and Pisa.

References

Allard P, Carbonnelle J, Métrich N, Loyer H, Zettwoog P (1994) Sulphur output and magma degassing budget of Stromboli volcano. Nature 368:326–330

Barberi F, Gandino A, Gioncada A, La Torre P, Sbrana A, Zenucchini C (1994) The deep structure of the Eolian arc (Filicudi-Panarea-Vulcano sector) in light of gravity, magnetic and volcanological data. J Volcanol Geotherm Res 61:189–206

Barker DS (1987) Rhyolites contaminated with metapelite and Gabbro, Lipari, Aeolian Islands, Italy: products of lower crustal fusion or of assimilation plus fractional crystallization? Contrib Mineral Petrol 97:460–472

Bence A E, Albeee L (1968) Empirical correction factors for the electron microanalysis of silicates and oxides. J Geol 76:382–402

Bodnar RJ, Reynolds TJ, Kuehn CA (1985) Fluid-inclusion systematic in epithermal systems. Rev Econ Geol 2:73–97

Bonaccorso A, Cardaci C, Coltelli M, Del Carlo P, Falsaperla S, Panucci S, Pompilio M, Villari L (1996) Annual report of the world volcanic eruptions in 1993, Stromboli. Bull Volcanic Eruptions 33:7–13

Burke EAJ, Lustenhouver WJ (1987) The application of a multichannel laser Raman microprobe (Microdil-28) to the analysis of fluid inclusions. Chem Geol 61:11–17

Caggianelli A, Del Moro A, Paglionico A, Piccareta G, Pinarelli L, Rottura A (1991) Lower crustal granite genesis connected with chemical fractionation in the continental crust of Calabria (southern Italy). Eur J Mineral 3:159–180

De Astis G, La Volpe L, Peccerillo A, Civetta L (1997) Volcanological and petrological evolution of Vulcano island (Aeolian Arc, southern Tyrrhenian Sea). J Geophys Res 102(b4):8021–8050

Del Moro A, Paglionico A, Piccarreta G, Rottura A (1986) Tectonic structure and Post-hercynian evolution of the Serre, Calabrian Arc, Southern Italy: geological, petrological and radiometric evidences. Tectonophysics 124:223–238

Esperança S, Crisci GM, De Rosa R, Mazzuoli R (1992) The role of the crust in the magmatic evolution of the Island of Lipari (Aeolian Islands, Italy) Contrib Mineral Petrol 112:450–462

Francalanci L (1997) Volcanological features of the Aeolian Islands, Southern Tyrrhenian Sea, Italy. In: Cortini M, De Vivo B, Livadie C (eds) Volcanism and archaelogy in Mediterranean Area. Research Signpost, Trivandrum, Kerala, India, pp 107–128

Francalanci L, Santo AP (1993) Magmatological evolution of Filicudi volcanoes, Aeolian Islands, Italy: constraints from mineralogical, geochemical and isotopic data. Acta Vulcanologica 3:203–227

Francalanci L, Barbieri M, Manetti P, Peccerillo A, Tolomeo L (1988) Sr-isotopic systematics in volcanic rocks from the island of Stromboli (Aeolian arc). Chem Geol 73:164–180

Francalanci L, Manetti P, Peccerillo A (1989) Volcanological and magmatological evolution of Stromboli volcano (Aeolian islands): the roles of fractional crystallisation, magma mixing, crustal contamination and source heterogeneity. Bull Volcanol 51:355–378

Francalanci L, Manetti P, Peccerillo A, Keller J (1993) Magmatological evolution of the Stromboli volcano (Aeolian Arc, Italy): inferences from major and trace element and Sr-isotopic composition of lavas and pyroclastic rocks. Acta Vulcanologica 3:127–151

Francalanci L, Tommasini S, Conticelli S, Davies GR (1999) Sr isotope evidence for short magma residence time for the 20th century activity at Stromboli volcano, Italy. Earth Planet Sci Lett 167:61–69

Frezzotti ML, Peccerillo A, Zanon V, Bonelli R (2002) Modeling of magma ascent beneath the Aeolian Islands: fluid inclusion studies in quartz-rich xenoliths. In: Coll Int Mount Pelée 1902-2002 Explosive Volcanism in Subduction Zones, 12–16 May 2002, Ile de la Martinique. G Aubert, Paris, Program Abstr 59

Gasparini C, Iannaccone G, Scandone P, Scarpa R (1982) Seismotectonics of Calabrian Arc. Tectonophysics 4:267–286

Gibert F, Guillaume D, Laporte D (1998) Importance of fluid immiscibility in the H2O-NaCl-CO2 system and selective CO2 entrapment in granulites: experimental phase diagram at 5-7 kbar, 900 °C and wetting textures. Eur J Mineral 10:1109–1123

Giberti G, Jaupart C, Sartoris G (1992) Steady-state operation of Stromboli volcano, Italy: constraints on the feeding system. Bull Volcanol 54:535–541

Gillot PY, Keller J (1993) Radiochronological dating of Stromboli. Acta Vulcanologica 3:69–77

Harris JL, Stevenson DS (1997a). Magma budgets and steady-state activity of Vulcano and Stromboli. Geophys Res Lett 24:1043–1046

Harris JL, Stevenson DS (1997b) Thermal observations of degassing open conduits and fumaroles at Stromboli and Vulcano using remotely sensed data. J Volcanol Geotherm Res 76:175–198

Herms P, Schenk V (1992) Fluid inclusions in granulite-facies metapelites of Hercynian ancient lower crust of the Serre, Calabria, Sourthern Italy. Contrib Mineral Petrol 112:393–404

Honnorez J, Keller J (1968) Xenolithe in vulkanischen Gesteiner der Aoliaschen Inseln (Sizilien). Geol Rundsch 57:719–736

Hornig-Kjarsgaard I, Keller J, Koberski U, Stadlbauer E, Francalanci L, Lenhart R (1993) Geology, stratigraphy and volcanological evolution of the island of Stromboli, Aeolian arc, Italy. Acta Vulcanologica 3:21–68

Johnston-Lavis HJ (1893) Enclosures of quartz in lava of Stromboli and changes in composition produced by them. Q J Geol Soc Lond Proc 55

Kerrick DM, Jacobs GK (1981) A modified Redlich-Kwong equation for H2O-CO2 mixtures at elevated pressures and temperatures. Am J Sci 281:735–767

Knott SD, Turco E (1991) Late Cenozoic kinematics of the Calabrian arc, southern Italy. Tectonics 10(6):1164–1172

Kretz R (1983) Symbols for rock-forming minerals. Am Mineral 68:277–279

Luth WC, Jahns RH, Tuttle OF (1964) The granite system at pressures of 4 to 10 kilobars. J Geophys Res 69:759–773

Maccarone E, Paglionico A, Piccareta G, Rottura A (1983) Granulite-amphibolite facies metasediments from the Serre (Calabria, southern Italy): their protoliths and the processes controlling their chemistry. Lithos 16:95–111

McKenzie DP (1972) Active tectonics of the Mediterranean region. Geophys J R Astron Soc 30:109–185

Metrich N, Clocchiatti R (1989) Melt inclusions investigation of the volcanic behaviour in historic basaltic magmas of Etna. Bull Volcanol 51:131–144

Morelli C, Giese P, Cassinis R, Colombi B, Guerra I, Luongo G, Scarascia S, Schutte KG (1975) Crustal structure of Southern Italy. A seismic refraction profile between Puglia-Calabria-Sicily. Boll Geofis Teor Appl 18:183–210

Peccerillo A, Kempton PD, Harmon RS, Wu TW, Santo AP, Boyce AJ, Tripodo A (1993) Petrological and geochemical characteristics of the Alicudi Volcano, Aeolian Islands, Italy: implications for magma genesis and evolution. Acta Vulcanologica 3:235–249

Pezzino A, Scribano V (1989) Notizie petrografiche e petrolchimiche sugli inclusi sialici e femici del neck di Strombolicchio (Stromboli). Boll Acc Gioenia Sci Nat 335:145–162

Ripepe M, Rossi M, Saccorotti G (1993) Image processing of explosive activity at Stromboli. J Volcanol Geotherm Res 54:335–351

Roedder E (1984). Fluid inclusions. Mineral Soc Am Rev Mineral 12:1–644

Rosi M, Bertagnini A, Landi P (2000) Onset of the persistent activity at Stromboli Volcano (Italy). Bull Volcanol 62:294–300

Schenk V (1980) U-Pb and Rb-Sr radiometric dates and their correlation with metamorphic events in the granulite-facies basement of the Serre, southern Calabria (Italy). Contrib Mineral Petrol 73:23–38

Schenk V (1989) P-T-t path of the lower crust in the Hercynian fold belt of southern Calabria. In Daly JS, Cliff RA, Yardley BW (eds) Evolution of metamorphic belts. Geol Soc Spec Publ 43:337–342

Schenk V (1990) The exposed crustal cross section of southern Calabria, Italy: structure and evolution of a segment of Hercynian crust. In: Salisbury MH, Fountain DM (eds) Exposed cross-section of the continental crust. Kluwer, Dordrecht, pp 21–42

Shaw HR (1963) The four-phase curve sanidine-quartz-liquid-gas between 500 and 4000 bars. Am Mineral 48:883–896

Thiery R, Van Den Kerkhof AM, Dubessy J (1994) *v*X properties of CH4-CO2 and CO2-N2 fluid inclusions: modelling for T<31 °C and P<400 bars. Eur J Mineral 6:753–771

Tuttle OF, Bowen NL (1958) Origin of granite in the light of experimental studies in the system NaAlSi3O8-KAiSi3O8-SiO2-H2O. Geol Soc Am Mem 74

Vaggelli G (1992) Lo studio delle inclusioni fluide come strumento di indagine magmatologica: applicazioni alle lave del Vesuvio e dello Stromboli. PhD Thesis, Dipartimento di Scienze della Terra, Universita' degli Studi di Firenze

Vaggelli G (1993) Silicate-melt inclusions as a tool for magmatological studies: application to Vesuvius and Stromboli lavas. Plinius 9:153–156

Vaggelli G, Belkin HE, Francalanci L, Manetti P (1991) Fluid inclusions in quartz xenocrysts of calc-alcaline rocks of Stromboli volcano, Italy. Plinius 5:231

Vaggelli G, Belkin HE, Francalanci L (1993). Silicate-melt inclusions in rocks from Stromboli volcano: a contribution to the understanding of the magmatic processes. Acta Vulcanologica 3:115–125

Vaggelli G, Olmi F, Conticelli S (1999) Quantitative electron microprobe analysis of reference silicate mineral and glass samples. Acta Vulcanologica 11:297–303

Vityk MO, Bodnar RJ (1995) Textural evolution of Synthetic fluid inclusions in quartz during reequilibration, with application to tectonic reconstruction. Contrib Mineral Petrol 121:309–323

Vityk MO, Bodnar RJ (1998) Statistical microthermometry of synthetic fluid inclusions in quartz during decompression re-equilibration. Contrib Mineral Petrol 13:149–162

Watson EB, Brenan JM (1987) Fluids in the lithosphere. 1. Experimentally-determined wetting characteristics of CO2-H2O fluids and their implications for fluid transport, host-rock physical properties and fluid inclusion formation. Earth Planet Sci Lett 85:497–515

Winkler HGF (1978) Come possiamo capire i magmi granitici? Soc Italiana Mineral Petrol Mus Storia Nat, pp 1–60

Zanon V (2001). Fluid and melt inclusions in quartz-rich xenoliths from the Aeolian Island: magmatological and volcanological implications. Plinius 25:105–110

Zvi Ben Avrahm, Boccaletti M, Cello G, Grasso M, Lentini F, Torelli L, Tortorici L (1987) Principali domini strutturali originatisi dalla collisione neogenico-quaternaria nel Mediterraneo centrale. Mem Soc Geol It 45:453–462